GBE

Genome Biology and Evolution

SMBE

Different Ancestries of R Tailocins in Rhizospheric *Pseudomonas* Isolates

Maarten G.K. Ghequire[1,*], Yörg Dillen[2], Ivo Lambrichts[2], Paul Proost[3], Ruddy Wattiez[4], and René De Mot[1]

[1]Centre of Microbial and Plant Genetics (CMPG), University of Leuven, Heverlee, Belgium

[2]Group of Morphology, Biomedical Research Institute (BIOMED), Hasselt University, Diepenbeek, Leuven, Belgium

[3]Laboratory of Molecular Immunology, Department of Microbiology and Immunology, Rega Institute, University of Leuven, Belgium

[4]Proteomics and Microbiology Laboratory, Research Institute for Biosciences, University of Mons, Mons, Belgium

*Corresponding author: E-mail: maarten.ghequire@biw.kuleuven.be.

Accepted: September 10, 2015

Data deposition: This project has been deposited at GenBank under the accession numbers KP698091, KP698092, and KP698093.

Abstract

Bacterial genomes accommodate a variety of mobile genetic elements, including bacteriophage-related clusters that encode phage tail-like protein complexes playing a role in interactions with eukaryotic or prokaryotic cells. Such tailocins are unable to replicate inside target cells due to the lack of a phage head with associated DNA. A subset of tailocins mediate antagonistic activities with bacteriocin-like specificity. Functional characterization of bactericidal tailocins of two *Pseudomonas putida* rhizosphere isolates revealed not only extensive similarity with the tail assembly module of the *Pseudomonas aeruginosa* R-type pyocins but also differences in genomic integration site, regulatory genes, and lytic release modules. Conversely, these three features are quite similar between strains of the *P. putida* and *Pseudomonas fluorescens* clades, although phylogenetic analysis of tail genes suggests them to have evolved separately. Unlike *P. aeruginosa* R pyocin elements, the tailocin gene clusters of other pseudomonads frequently carry cargo genes, including bacteriocins. Compared with *P. aeruginosa*, the tailocin tail fiber sequences that act as specificity determinants have diverged much more extensively among the other pseudomonad species, mostly isolates from soil and plant environments. Activity of the *P. putida* antibacterial particles requires a functional lipopolysaccharide layer on target cells, but contrary to R pyocins from *P. aeruginosa*, strain susceptibilities surpass species boundaries.

Key words: bacteriocin, phage tail, antibacterial, pyocin.

Introduction

Bacteria are able to secrete very diverse secondary metabolites and ribosomally synthesized antimicrobials to antagonize competitors with similar niche preferences. Molecular sizes of these antibacterials vary largely, ranging from small peptides to multiprotein complexes (Hibbing et al. 2010). Historically, the (poly)peptides which exhibit high specificity and selectively kill close phylogenetic relatives of the producer are collectively referred to as bacteriocins. In recent years, it has become clear that bacteriocin-like activity of Gram-negative bacteria can also be mediated by type VI secretion substrates, proteins causing contact-dependent inhibition, or Rhs (rearrangement hot spot) proteins (Braun and Patzer 2013; Ruhe et al. 2013; Durand et al. 2014; Hayes et al. 2010, 2014; Russell et al. 2014).

The *Escherichia coli* colicins and the *Pseudomonas aeruginosa* pyocins are among the best-characterized "classical" bacteriocins of Gram-negative bacteria. In the latter species, five types have been described (Ghequire and De Mot 2014). S-type pyocins are bacteriocins with a modular organization similar to colicins. They consist of a receptor-binding domain typically targeting outer membrane receptors involved in iron uptake (Baysse et al. 1999; Denayer et al. 2007; Elfarash et al. 2012, 2014), a translocation domain, and a carboxy-terminal toxin domain with nuclease or pore-forming activity. Self-intoxication of a producer is prevented by tightly regulated coexpression of an immunity gene (Ghequire and De Mot 2014). Such accessory immunity partner appears not to be required for lipid II-degrading M-type pyocins that cause inhibition of peptidoglycan biosynthesis similarly to colicin

M (Barreteau et al. 2012). L pyocins carrying a tandem of lectin domains have no counterpart among colicins (Ghequire et al. 2014; McCaughey et al. 2014). The carboxy-terminal lectin domain, recognizing D-rhamnose, allows anchoring onto the cellular surface (McCaughey et al. 2014), but target specificity is mainly conferred by the amino-terminal domain (Ghequire et al. 2013).

Two morphologically distinct types of bactericidal "tailocins", high-molecular-weight (HMW) bacteriocins showing structural similarities with bacteriophage tails, have been described in *P. aeruginosa* (Michel-Briand and Baysse 2002). The R-type pyocins are rigid and contractile, whereas the F-type pyocins are flexible but noncontractile. Based on gene cluster similarities, a common ancestry with tailed enterobacteriophage, P2 (*P2likevirus* genus of the *Myoviridae* family) for the R-type and with phage λ (*Lambdalikevirus* genus of the *Siphoviridae*) for the F-type, was proposed by Nakayama et al. (2000). To date, five R-type and three F-type pyocins have been described (Ghequire and De Mot 2014). Although the F pyocin receptors remain unrevealed, it was demonstrated that an L-rhamnose and two D-glucose residues of the lipopolysaccharide (LPS) outer core account for the O-serotype-specific character of susceptibility for R1, R2, and R5 pyocins, respectively (Köhler et al. 2010). In the case of pyocin R3, a glucose residue in the core oligosaccharide is involved in bacteriocin susceptibility as well. A deletion in the *wapB* promoter prevents the addition of this terminal carbohydrate residue and accounts for bacteriocin resistance (Kocíncová and Lam 2013). Atomic-resolution structures of pyocin R2 in extended configuration (sheath and tube) and in the contracted state (sheath) obtained by cryo-electron microscopy suggest a possible mechanism for release of stored energy to drive perforation of bacterial membranes by the inner tube (Ge et al. 2015). With its inner surface being lined by negative charges, the tube then functions as a cation-conducting channel that dissipates the proton potential of the target cell.

The expression of *P. aeruginosa* S-type, R-type, and F-type pyocin genes is controlled by the PrtN activator that binds to regulatory P boxes in their promoter regions. In noninducing conditions, expression of *prtN* is repressed by PrtR. Upon exposure to stress conditions, such as DNA damage by chemicals or UV irradiation, activated RecA triggers auto-proteolytic cleavage of PrtR, which abrogates *prtN* repression and leads to pyocin production (Ghequire and De Mot 2014). RecA-mediated pyocin production can also be triggered by the CRISPR/Cas phage immunity system in sessile *P. aeruginosa* cells (Heussler et al. 2015). Under denitrifying conditions, pyocins are enclosed within *P. aeruginosa* membrane vesicles, equally dependent on the SOS response route (Toyofuku et al. 2014). The *P. aeruginosa prtR* and *prtN* genes are located upstream of the pyocin clusters, in opposite orientation (Ghequire and De Mot 2014). PrtR also binds its own promoter, pointing to autorepressive regulation and resulting in relatively stable PrtR expression levels (Sun et al. 2014). In addition, PrtR also controls expression of *ptrB*, encoding a Type III secretion system repressor, which is located in opposite direction of *prtR* just ahead of the pyocin cluster (Wu and Jin 2005).

Also in soil-dwelling and plant-associated pseudomonads different types of bacteriocins, often subject to stress-induced production, have been characterized: Pyocin M homologs in *Pseudomonas fluorescens* and pathovars of *Pseudomonas syringae* (Barreteau et al. 2009; Grinter et al. 2012); L-type bacteriocins in *Pseudomonas protegens*, *Pseudomonas putida* and *P. syringae* (Parret et al. 2003, 2005; de los Santos et al. 2005; Ghequire et al. 2012); a gyrase-inhibiting B-type microcin in *P. syringae* (Metelev et al. 2013); and a phage tail-like bacteriocin in *P. fluorescens* SF4c (Fischer et al. 2012). Using hybridization of genomic DNA from 30 *P. fluorescens* strains with DNA probes derived from P2-like tail genes in *P. fluorescens* SBW25 and λ-like tail genes in *P. fluorescens* Q8r1-96, the widespread occurrence, either individually or combined, of such phage-like genes was demonstrated (Mavrodi et al. 2009). Comparative genomics of the *P. fluorescens* clade revealed that in most strains the *mutS–cinA* intergenic region is occupied by mosaic P2- and/or λ-type phage-related clusters differing in size and gene composition, but their exact nature (intact prophage or remnant, HMW bacteriocin) remains elusive (Loper et al. 2012).

In this study we characterized HMW bacteriocins in two *P. putida* strains, isolated from the rhizosphere of banana (strain BW11M1) and rice (strain RW10S2), and identified the corresponding gene clusters. Phylogenetic analysis of regulatory, tail assembly and lysis genes of HMW bacteriocins and related (pro)phages was used to acquire insight in the diversity and ancestry of these mobile elements ubiquitously present in pseudomonad genomes. Based on this genomic perspective we propose a phylogeny-based classification of R tailocins in pseudomonads.

Materials and Methods

Strains, Media, and Growth Conditions

Bacterial strains used in this study are listed in table 1. *Pseudomonas* strains were cultured in Tryptic Soy Broth (TSB 3%, BD Biosciences) at 30 °C, on a rotary shaker at 200 rpm. *Escherichia coli* and *P. aeruginosa* strains were grown at 37 °C in LB (2.5%; MP Biomedicals). Media were solidified with 1.5% agar (Invitrogen) and supplemented with kanamycin (50 μg/ml; Sigma-Aldrich) or spectinomycin (100 μg/ml; Sigma-Aldrich) when required.

Genomic DNA from *Pseudomonas* strains was extracted using the Puregene Yeast/Bact. Kit B (Qiagen). Plasmid DNA was isolated using the QIAprep Spin Miniprep Kit (Qiagen). Bacterial stocks were stored in the appropriate medium at −80 °C in 25% (v/v) glycerol (VWR International).

Large-Scale Production and Purification of R Tailocin

One-milliliter volumes of overnight test tube cultures of *P. putida* BW11M1 were transferred to 500 ml erlenmeyers. After the OD_{600} reached 0.5, filter-sterilized mitomycin C (Sigma-Aldrich) was added to a final concentration of 0.1 μg/ml. The culture was incubated further until cell lysis occurred. Subsequently, benzonase nuclease (2 U/ml; Sigma-Aldrich) was added to the lysed culture to reduce the viscosity, followed by a 30-min incubation at 37 °C. Debris and membrane fragments were removed by centrifugation at 8,000 × g for 30 min at 4 °C. Supernatants were filter sterilized (0.22 μm; Millipore) and supplemented with polyethylene glycol (PEG) 6000 (Sigma-Aldrich) and NaCl (VWR International) at final concentrations of 10% (w/v) and 0.5 M, respectively. This mixture was stirred overnight (200 rpm, 4 °C) and centrifuged the following day at 8,000 × g for 1 h at 4 °C. The precipitate was resuspended in 10 ml TN50 buffer (50 mM NaCl, Tris–HCl 10 mM, pH 7.5) and centrifuged at 4,000 × g for 15 min at 4 °C to remove small undissolved debris. Finally, bacteriocin particles were sedimented at 48,400 × g for 3 h at 4 °C, resuspended in 2 ml TN50 buffer and filtered (0.45 μm; Millipore) and further purified by gel filtration using a Sephacryl S-500 HR column (16/60, GE Healthcare Life Sciences; fractionation range for dextrans: $4 \times 10^4 - 2 \times 10^7$ Da) at an elution rate of 0.7 ml/min. Collected fractions were tested for antibacterial activity and analyzed by transmission electron microscopy, SDS-PAGE (sodium dodecyl sulfate polyacrylamide gel electrophoresis), and mass spectrometry. Bacteriocin samples were kept at 4 °C until use.

Transmission Electron Microscopy

Purified tailocins from *P. putida* BW11M1 were transferred to 0.7% formvar-coated copper grids (Aurion, Wageningen, The Netherlands) by placing the grids in the tailocin emulsion for 30 s. Consequently, the tailocins were incubated in 0.25% phosphotungstenic acid (pH 7) for 30 s at room temperature and washed in distilled water. After sample drying, analysis was performed with a Phillips EM208 S transmission electron microscope (80 kV), equipped with a Morada Soft Imaging System camera. Digital processing of the obtained images was performed with the iTEM-FEI software (Olympus SIS, Münster, Germany).

Bacteriocin Assay

Spot activity assays with purified tailocins from *P. putida* BW11M1 and RW10S2, and extracts of derived tailocin mutants, were performed as follows. First, cell lawns were prepared by overlaying TSA (Tryptic Soy Agar) plates with 5 ml of TSB soft agar (0.5 %), seeded with 25 μl of the indicator strain (~10^8 CFU/ml). Next, 10 -μl volumes of collected bacteriocin were spotted on top of these plates and allowed to air-dry. Heat sensitivity of the purified bacteriocins was tested by heating the tailocins in a heat block at 75 °C for 10 min. After cooling to room temperature, samples were spotted onto cell lawns as described above. Plates were incubated overnight at 30 °C (37 °C for *P. aeruginosa*). The following day, plates were evaluated for the presence of halos. TN50 buffer was used as a negative control.

Protein Electrophoresis and Amino-Terminal Amino Acid Sequencing

Samples with bacteriocin activity collected after gel filtration chromatography were analyzed through SDS-PAGE (Invitrogen) at 200 V for 0.7 h using the Precision Plus Protein Kaleidoscope ladder (Bio-Rad) as a size standard. After separation, the gels were electroblotted onto polyvinylidene difluoride (PVDF) membranes (Invitrogen) and stained with Coomassie blue R-250 (Bio-Rad) to visualize proteins. Protein bands were cut from the membrane, destained in methanol (VWR International) and amino-terminal sequencing was performed by automated Edman degradation, using a Procise 491 cLC protein sequencer (Applied Biosystems, Foster City, CA).

Recombinant DNA Methods

Standard methods were used for the preparation of competent *E. coli* and *P. putida* cells, heat shock transformation of *E. coli* and DNA electrophoresis (Green and Sambrook 2012). SMART ladder (Eurogentec) was used as a standard for DNA size estimation. Restriction enzymes were used according to the supplier's specifications (Roche Diagnostics). DNA ligation was performed using T4 DNA ligase (Invitrogen). Sequencing of plasmid DNA was performed by GATC Biotech (Constance, Germany).

Construction of Tailocin Mutants

Terminal regions of *ptbJ* (encoding phage tail sheath protein) and *ptbF* (encoding baseplate protein) from the R tailocin gene clusters of *P. putida* BW11M1 and RW10S2, respectively, were amplified by polymerase chain reaction (PCR) with *Pfx* DNA polymerase (Invitrogen), using genomic DNA as a template. Primers used are listed in supplementary table S1, Supplementary Material online. Amplicons were purified with the QIAquick PCR Purification kit (Qiagen), digested with *Hin*dIII and *Bam*HI for the upstream, and *Bam*HI and *Eco*RI for the downstream fragments, and subsequently ligated in suicide plasmid pAKE604 (El-Sayed et al. 2001). Sequence-verified plasmids pCMPG6226 and pCMPG6227, carrying the fused upstream and downstream fragments of BW11M1 *ptbJ* and RW10S2 *ptbF*, respectively, were transformed to *E. coli* S17-1 λpir and transferred to the corresponding *P. putida* strains through biparental conjugation. Selection with kanamycin and spectinomycin yielded transformants that were individually grown in a test tube without antibiotic for 12 h. Serial dilutions were plated out on TSA containing

Table 1

Susceptibility of *Pseudomonas* Species Groups to R Tailocins of *Pseudomonas putida* Strains BW11M1 and RW10S2

Species	Strain	Genotype/Characteristics	Susceptibility to Tailocin R_{BW11M1}	Susceptibility to Tailocin R_{RW10S2}	Origin or Reference
Pseudomonas aeruginosa	PA14	Opportunistic pathogen, human isolate	–	–	*Pseudomonas* genome DB
Pseudomonas aeruginosa	PAO1	Opportunistic pathogen, human isolate	–	–	*Pseudomonas* genome DB
Pseudomonas agarici	LMG 2112	Mushroom isolate, type strain	–	–	BCCM collection
Pseudomonas aureofaciens	LMG 1245	River clay, type strain	–	–	BCCM collection
Pseudomonas chlororaphis	LMG 5004	Contaminated plate, type strain	–	–	BCCM collection
Pseudomonas cichorii	LMG 2162	*Cichorium*, type strain	–	–	BCCM collection
Pseudomonas entomophila	L48	Entomopathogenic strain that kills *Drosophila melanogaster*	–	+	*Pseudomonas* genome DB
Pseudomonas fluorescens	13-79	Wheat rhizosphere	–	–	Weller and Cook (1983)
Pseudomonas fluorescens	2-79	Wheat rhizosphere	–	–	Weller and Cook (1983)
Pseudomonas fluorescens	A506	Pear isolate	–	–	*Pseudomonas* genome DB
Pseudomonas fluorescens	BW11P2	Banana rhizosphere	+	–	Vlassak et al. (1992)
Pseudomonas fluorescens	DR54	Viscosinamide producer, sugar beet rhizosphere isolate	+	–	Nielsen et al. (1999)
Pseudomonas fluorescens	F113	Sugarbeet rhizosphere	–	–	*Pseudomonas* genome DB
Pseudomonas fluorescens	LMG 1794	Prefilter water-works tank, type strain	–	–	BCCM collection
Pseudomonas fluorescens	OE 28.3	Wheat rhizosphere	–	–	CMPG collection
Pseudomonas fluorescens	Pf0-1	Soil isolate	+	–	*Pseudomonas* genome DB
	CMPG2247	R_{BW11M1} tailocin-resistant Pf0-1 mutant	–	–	This study
	CMPG2248	R_{BW11M1} tailocin-resistant Pf0-1 mutant	–	–	This study
	CMPG2249	R_{BW11M1} tailocin-resistant Pf0-1 mutant	–	–	This study
	CMPG2250	R_{BW11M1} tailocin-resistant Pf0-1 mutant	–	–	This study
Pseudomonas fluorescens	SBW25	Sugar beet leaves	–	–	*Pseudomonas* genome DB
Pseudomonas fluorescens	WCS365	Potato rhizosphere	–	–	Geels and Schippers (1983)
Pseudomonas gingeri	LMG 5327t1	Mushroom, type strain	–	–	BCCM collection
Pseudomonas marginalis	LMG 2210	*Cichorium* isolate, pathovar reference strain	–	–	BCCM collection
Pseudomonas mendocina	LMG 1223	Isolate from ethanol-enriched soil	–	–	BCCM collection
Pseudomonas protegens	Pf-5	Soil isolate	–	–	*Pseudomonas* genome DB
Pseudomonas putida	GB-1	Fresh water isolate, manganese oxidizer	–	–	*Pseudomonas* genome DB
Pseudomonas putida	OE 47.1	Maize rhizosphere	–	–	CMPG collection
Pseudomonas putida	OE 53.2	Maize rhizosphere	–	–	CMPG collection
Pseudomonas putida	OE 55.1	Maize rhizosphere	–	–	CMPG collection
Pseudomonas putida	OE 55.7	Maize rhizosphere	–	–	CMPG collection
Pseudomonas putida	WCS358	Potato rhizosphere	–	–	*Pseudomonas* genome DB
Pseudomonas savastanoi	LMG 6768	*Nerium oleander* isolate	–	+	BCCM collection
Pseudomonas syringae	DC3000	Model pathogen, bacterial speck on tomato and *Arabidopsis*	–	+	*Pseudomonas* genome DB

(continued)

Table 1 Continued

Species	Strain	Genotype/Characteristics	Susceptibility to Tailocin R_{BW11M1}	Susceptibility to Tailocin R_{RW10S2}	Origin or Reference
Pseudomonas syringae	GR12-2R3	Grass rhizosphere	–	–	Lifshitz et al. (1987)
Pseudomonas syringae	LMG 1247	Isolate from *Syringa vulgaris*, pathovar reference strain	–	+	BCCM collection
Pseudomonas syringae	LMG 5192	*Nicotiana tabacum* isolate	–	+	BCCM collection
Pseudomonas syringae	LMG 5295	*Raphanus sativus* isolate	–	–	BCCM collection
Pseudomonas syringae	LMG 5456	*Cucumis sativus* isolate	–	+	BCCM collection
	CMPG2251	R_{RW10S2} tailocin-resistant LMG 5456 mutant	–	–	This study
	CMPG2252	R_{RW10S2} tailocin-resistant LMG 5456 mutant	–	–	This study
	CMPG2253	R_{RW10S2} tailocin-resistant LMG 5456 mutant	–	–	This study
	CMPG2254	R_{RW10S2} tailocin-resistant LMG 5456 mutant	–	–	This study
Pseudomonas tolaasii	CH36	Mushroom	–	–	CMPG collection
Pseudomonas tolaasii	LMG 2342	Mushroom, type strain	–	–	BCCM collection
Pseudomonas viridiflava	LMG 2352	*Phaseolus* sp. isolate, type strain	–	+	BCCM collection

Note.—"+," sensitive; "–," insensitive. *Pseudomonas* genome DB, *Pseudomonas* genome database (Winsor et al. 2011).

sucrose (7%; VWR International) to select for the loss of the cassette. Allelic exchanges of the recombinants were checked by PCR with Taq polymerase (BIOKÉ), using primers PGPRB-10022 and PGPRB-10025 for strain BW11M1, and PGPRB-10120 and PGPRB-10123 for strain RW10S2. Putative mutants were sequence verified for in-frame deletions following PCR amplification with *Pfx*. Resulting deletion mutants were CMPG2245 (deletion of internal 780-bp fragment of *ptbJ* in BW11M1) and CMPG2246 (deletion of internal 681-bp fragment of *ptbF* in RW10S2).

Generation of Spontaneous Tailocin Resistant Mutants

A bacteriocin assay was performed on 24-h-old cultures of R tailocin-susceptible strains Pf0-1 (for the BW11M1 R tailocin) and LMG 5456 (for the RW10S2 R tailocin), using the spot-on-lawn assay. After 48-h incubation, tailocin-resistant mutants can be isolated as colonies growing inside the tailocin halos. One mutant (if present) per halo per cell culture was streaked to single colony and verified for resistance to the tailocin by spot assay (Pf0-1 mutants CMPG2247–CMPG2250; LMG 5456 mutants CMPG2251–CMPG2254). To exclude the isolation of bacteriocin-tolerant contaminant bacteria, genomic DNA of the presumed mutants was isolated and the boxA element was amplified using primer BOXA1R (PGPRB-10181; supplementary table S1, Supplementary Material online) as described (Koeuth et al. 1995). After gel electrophoresis, the banding patterns of the wild-type strains and resistant mutants were compared.

LPS Purification and SDS-PAGE Analysis

LPS was prepared by the method of Hitchcock and Brown (1983). Briefly, overnight bacterial cultures were diluted to OD_{600} 0.5 and washed twice with phosphate-buffered saline (Sigma-Aldrich). Cell pellets of wild-type strains and resistant mutants were dissolved in 250 µl Hitchcock and Brown lysis buffer (SDS 20 mg/ml [Sigma-Aldrich], glycerol 10% v/v, bromophenol blue 0.02 mg/ml [Sigma-Aldrich], 1 M Tris–HCl [Invitrogen] pH 6.8), and heated at 100 °C for 30 min. After cooling, 1.5-µl volumes of proteinase K (20 mg/ml; Sigma-Aldrich) were added and the mixtures incubated overnight at 55 °C. The following day, the samples were heated for 5 min at 100 °C before loading 5-µl volumes on the gel for SDS-PAGE analysis. Gels were electrophoresed for 1 h at 150 V and LPS was visualized with the SilverQuest Silver Staining Kit (Invitrogen) using the basic staining protocol.

Liquid Chromatography-Tandem Mass Spectrometry Analysis

The identification of proteolytic peptides resulting from in-solution digestion of HMW fractions was performed on an UHPLC-HRMS (ultra-high-pressure liquid chromatography - high resolution mass spectrometry) platform combining a NanoLC-Ultra system (Eksigent) with a TripleTOF 5600 System (AB SCIEX). Tryptic peptides were separated in a 25-cm C18 reverse-phase column (Acclaim PepMap 100, 3 µm; Dionex) by a linear acetonitrile gradient (4–35% v/v, flow rate of 300 nl/min, 20 min) in water containing 0.1% (v/v) formic acid. The time-of-flight analyzer was regularly and

automatically calibrated with tryptic peptides of β-galactosidase from *E. coli*, which maintains an average mass error below 10 ppm across all injections. Mass spectra (MS) were acquired across 400–1,500 m/z with 0.5-s accumulation time. A maximum number of 50 precursors per cycle was selected according to an intensity threshold of 200 counts per second. Each selected precursor was accumulated for 50 ms and submitted to fragmentation with N_2 as the collision gas. Tandem mass spectrometry (MS/MS) spectra were acquired across 100–1,800 m/z and an exclusion time of 30 s was applied. The acquired data were analyzed using ProteinPilot Software v. 4.1 (AB SCIEX) and searched against the UniProt TrEMBL database or a local database covering the BW11M1 (Li et al. 2013) and RW10S2 (Rokni-Zadeh et al. 2012) genomes. The search parameters included aminocarbamidomethyl cysteine, all biological modifications and amino acid (AA) substitutions, and one missed trypsin cleavage. Sequenced peptides (95%) represent the number of distinct peptides having at least 95% confidence. Multiple modified and cleaved states of the same underlying peptide sequence are considered distinct peptides due to different molecular formulas. Sequence coverage (95%) corresponds to the percentage of matching AAs from identified peptides having confidence greater than or equal to 95%, divided by the total number of AAs in the sequence.

Phylogenetic Analysis

The predicted AA sequences of the *P. putida* BW11M1 and RW10S2 tail proteins (PtbJ, PtbK, and PtbH), lysis proteins (PtbB and PtbR), and regulator protein (PtbA) were used as BLAST (Basic Local Alignment Search Tool) homology search queries against the nonredundant protein database and draft genomes of pseudomonads to identify and delineate related tailocin gene clusters and prophages. The same approach was used to screen bacteriophage genomes (subset *Caudovirales*) for distant homologs. Sequence alignments and phylogenetic analyses were performed with Geneious 7.1.7 (http://www.geneious.com). Synteny between related gene clusters was evaluated by pairwise and multiple alignment using MAFFT v7.017 (Katoh and Standley 2013). Complete multiple alignments of AA sequences performed with MUSCLE (implemented in Geneious 7.1.7) were used to construct maximum-likelihood trees using PhyML (JTT [Jones, Taylor, and Thorton] substitution model; version 2.2.0) (Guindon and Gascuel 2003). The following settings were used for PhyML (implemented in Geneious 7.1.7): Estimated proportion of variable sites, optimization of topology/length/rate, best topology of NNI and SPR searches. For identification and classification of predicted holins, homology searches were conducted against the Transporter Classification (TC) database (http://www.tcdb.org). Protein domains were localized using SMART (http://smart.embl-heidelberg.de/) and InterPro (https://www.ebi.ac.uk/interpro) analyses.

Genome Sequencing and Nucleotide Accession Numbers

GenBank accession numbers of the nucleotide sequences of the R tailocin clusters from *P. putida* strain BW11M1, RW10S1 and RW10S2 are KP698091, KP698092 and KP698093, respectively.

Results

Strain-Specific Antibacterial Activities of Phage-Related Complexes Purified from Two *P. putida* Rhizosphere Isolates

Pseudomonas putida strain BW11M1 produces a 30-kDa lectin (LlpA) with bacteriocin activity against a number of fluorescent pseudomonads (Ghequire et al. 2012), and the cyclic lipopeptide xantholysin that inhibits the growth of several xanthomonads and fungi (Li et al. 2013). The culture supernatant of this strain also shows antagonistic activity against some *Pseudomonas* isolates that are insensitive to LlpA and xantholysin, suggesting that BW11M1 is capable of producing at least one other, yet unidentified anti-*Pseudomonas* substance. This antagonistic effect was abolished upon heat treatment of the culture supernatant (see further) and, compared with LlpA, resulted in relatively small inhibition zones which are typically observed for large, slowly diffusing inhibitory protein complexes such as phage-like bacteriocins (Ghequire and De Mot 2014).

Increased production of the presumed bacteriocin activity by strain BW11M1 was obtained by exposing the culture to mitomycin C, which was accompanied by cell lysis. After cellular debris removal, HMW particles were collected by PEG precipitation and subsequent gel filtration. SDS-PAGE analysis of this HMW bacteriocin-active fraction of *P. putida* BW11M1 revealed the presence of several proteins (fig. 1*A*). After blotting to a PVDF membrane, amino-terminal sequences of the most prominent bands were determined through Edman degradation. Peptide sequences matched to phage-like structural proteins (predicted tail sheath, baseplate, and tail tube protein) encoded by a *ptb* (phage tail-like bacteriocin) gene cluster identified in the draft genome of *P. putida* BW11M1 (fig. 2). Genomic regions highly similar to this cluster were also retrieved in the draft genomes of rice rhizosphere isolates *P. putida* RW10S1 (Li et al. 2011) and RW10S2 (Rokni-Zadeh et al. 2012). Of these, *P. putida* RW10S2 was equally examined for HMW bacteriocin production, resulting in an active particulate fraction with a protein banding pattern similar to the one observed for the purified BW11M1 sample (data not shown).

Activity of both bacteriocins was assayed against a diverse set of pseudomonad isolates by applying 10-µl spots of purified HMW complexes on trypticase soy agar plates, overlaid with soft agar seeded with cells of the respective indicator strains. After overnight incubation, plates were scored for the presence of growth inhibition halos (fig. 1*B* and *C*).

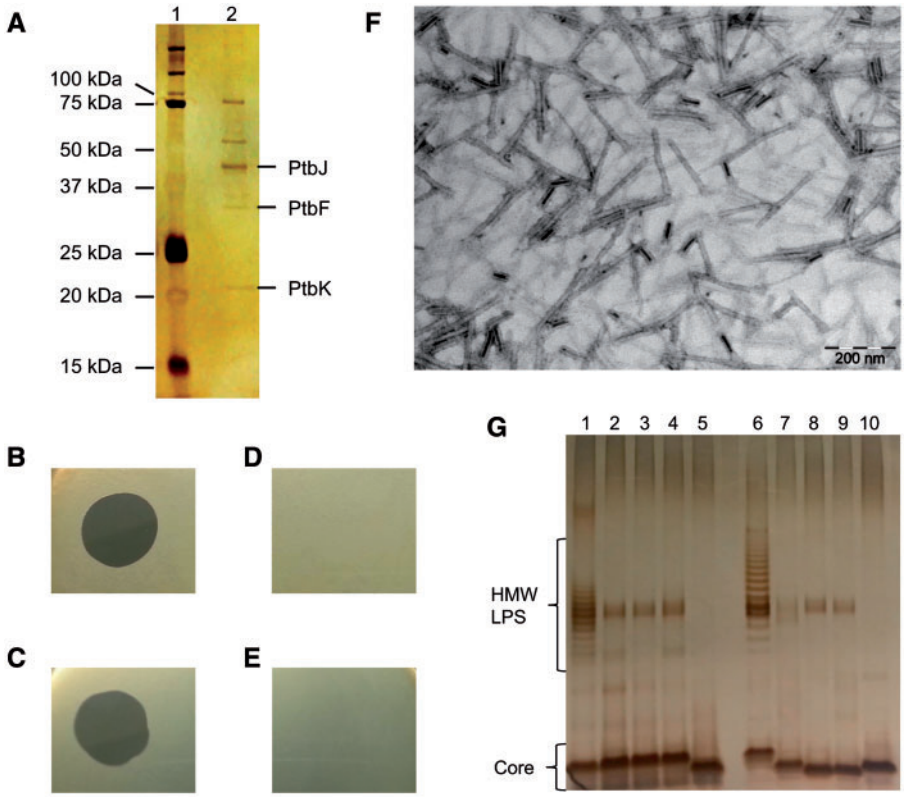

Fig. 1.—(*A*) Silver-stained SDS-PAGE gel of purified R tailocin from *P. putida* BW11M1. Lane 1, ladder with indicated sizes; lane 2, banding pattern of R particle with protein annotations resulting from amino-terminal sequencing. Sequences obtained were: SGFFHGVTVTNVDTGARSI, corresponding to PtbJ (~43 kDa, predicted size 41.8 kDa); S(Q)VDLSKLPA, corresponding to PtbF (~33 kDa, predicted size 31.8 kDa); AMIPETLANLNLFVD, corresponding to PtbK (~21 kDa, predicted size 18.3 kDa). (*B*–*E*) Antagonistic activity of tailocins. Spot-on-lawn assay of purified HMW extracts of (*B*) *P. putida* BW11M1, (*C*) *P. putida* RW10S2, (*D*) CMPG2245 (*ptbJ* mutant of BW11M1), (*E*) CMPG2246 (*ptbF* mutant of RW10S2) against indicator strains *P. fluorescens* Pf0-1 (*B* and *D*) and *P. syringae* LMG 5456 (*C* and *E*). (*F*) Electron microscopy structure of the R tailocin from *P. putida* BW11M1. Contracted particles are recognizable as electron-dense sheath-core regions. Average tailocin dimensions were 166.95 nm (length, SD: 32.73 nm; 65 particles) and 13.22 nm (width, SD: 2.74 nm; 72 particles) when in extended form, and 65.96 nm (length, SD: 11.18 nm; 43 particles) and 19.64 nm (width, SD: 2.94 nm; 44 particles) when contracted. The scale bar is indicated. (*G*) LPS profile of tailocin-susceptible wild-type strains and tailocin-resistant mutants. Extracted LPS was separated by SDS-PAGE and silver-stained. Lane 1, Pf0-1 wild-type; lanes 2–5, Pf0-1 mutants resistant to tailocin R_{BW11M1} (lanes 2–5: CMPG2247–CMPG2250); lane 6, LMG 5456 wild-type; lanes 7–10, LMG 5456 mutants resistant to tailocin R_{RW10S2} (lane 7–10: CMPG2251–CMPG2254).

The test panel consisted of a set of *Pseudomonas* culture collection strains, together with fluorescent *Pseudomonas* rhizosphere isolates from our own collection. Results are summarized in table 1. For the phage-like complex from strain BW11M1, 3 of 38 tested isolates proved to be susceptible, whereas 7 of them were killed by the protein complex from strain RW10S2, together covering about 26% of the strains tested. Susceptible strains belong to different species, including *P. fluorescens* and *P. syringae*, whereas no *P. putida* indicator was found. None of the strains was susceptible to both particles. As initially no sensitive *P. aeruginosa* strain could be identified, this species panel was expanded to strains belonging to 15 different O serotypes, but again no susceptible strain could be retrieved (data not shown).

To verify that the observed antagonistic activities are not caused by other copurified bacteriocins or phages, defined nonmarked BW11M1 and RW10S2 mutants were constructed by deletions in *ptbJ* and *ptbF*, respectively, that encode predicted structural proteins of the phage-like complexes (putative tail sheath protein and baseplate protein, respectively). The PEG-precipitated HMW fractions derived from culture supernatants of mitomycin-induced BW11M1 and RW10S2 *ptb* mutants did not display the wild-type antibacterial activity (fig. 1*D* and *E*), hereby confirming that the observed bacteriocin activities were solely attributable to the respective purified particles.

Biochemical Characterization Reveals LPS-Targeting R-Type Tailocins

Based on extensive gene synteny and significant AA sequence homologies of encoded proteins with the R-type pyocin

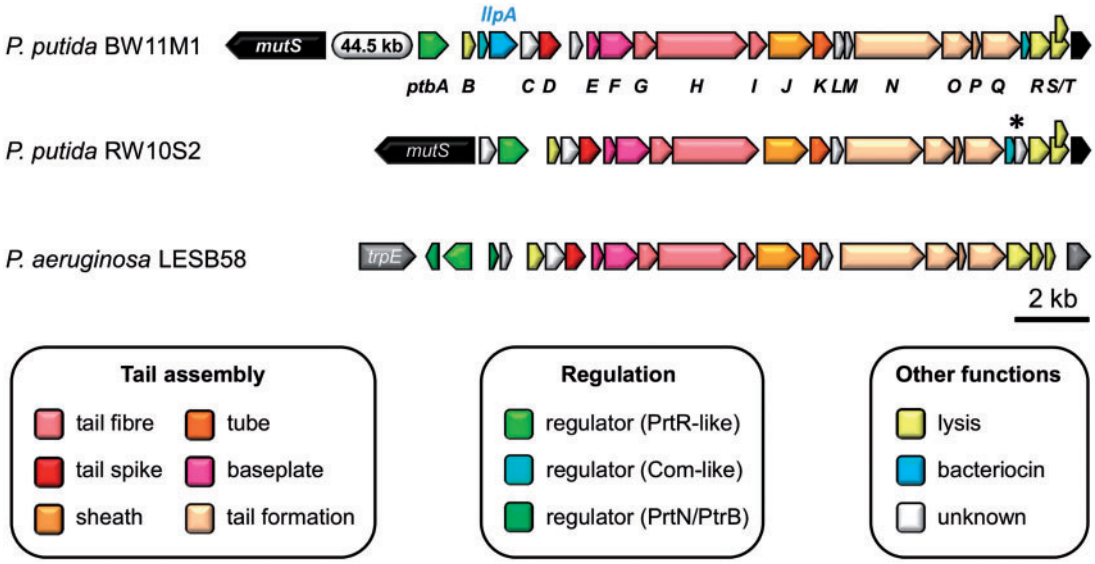

FIG. 2.—Gene organization of the R tailocin clusters from *P. putida* strains BW11M1 and RW10S2. The genomic region of strain LESB58 is included to illustrate synteny with a canonic R pyocin cluster from *P. aeruginosa*. Arrows represent coding regions which are colored according to their predicted function (color legend in boxes). Flanking gene pairs *mutS–cinA* (black) and *trpE–trpG* (gray) are included. The *ptb* genes are denoted *ptbA* through *ptbT*. The cargo genes of strains BW11M1 (bacteriocin LlpA) and RW10S2 (unknown; marked with asterisk) are highlighted. The scale bar represents a DNA region of 2,000 bp.

backbone of *P. aeruginosa* (fig. 2), the Ptb system likely represents an R-type of phage tail-like bacteriocin. This was further queried by analyzing the purified BW11M1 and RW10S2 particles through MS/MS. The samples were digested with trypsin and the resulting peptides were analyzed using an UHPLC-nanoESI-MS/MS approach. Multiple proteins were identified as *ptb* gene products encoding phage tail proteins: PtbC, PtbE, PtbF, PtbG, PtbH, PtbJ, PtbK, PtbN, PtbO, PtbP, and PtbQ (fig. 2, supplementary table S2, Supplementary Material online). In the RW10S2 sample, PtbL was detected as well. No indication was found for the possible presence of phage head compartment proteins.

Transmission electron microscopy on the purified HMW fraction of BW11M1 (fig. 1*F*) revealed structures consisting of a double cylinder, quite similar to previously obtained structures of R-type pyocins (Michel-Briand and Baysse 2002). Measured dimensions of the BW11M1 tail-like complexes or tailocins were 167 nm (length) and 13 nm (width) when sheaths are in extended form. Part of the complexes displaying higher electron density apparently represent contracted forms, resulting in thickened sheaths of 66 nm long and 20 nm wide. As compared with the *P. aeruginosa* pyocin R2 complexes studied by cryo-electron microscopy (Ge et al. 2015), slightly higher length and width ratios of uncontracted versus contracted sheaths are observed for the BW11M1 tailocin (2.53 vs. 2.4 and 1.48 vs. 1.3, respectively). As expected, bacteriocin activity of the BW11M1 and RW10S2 tailocins was lost after heat treatment, due to disassembly of the multiprotein complexes (data not shown).

To isolate spontaneous tailocin-resistant mutants, stationary phase cultures of *P. fluorescens* Pf0-1 and *P. syringae* LMG 5456 were subjected to spot-on-lawn assays with R_{BW11M1} and R_{RW10S2} particles, respectively. Colonies emerging inside the halos were picked, and bacteriocin resistance of these suspected mutants was confirmed by the absence of halos in a subsequent spot-on-agar test (table 1). Given the involvement of LPS in cellular killing by R pyocins, LPS banding profiles of the isolated clones were analyzed and compared with the wild-type indicator strains (fig. 1*G*). Major differences in the LPS patterns were observed, often in combination with altered constitution of the core regions, pointing toward the loss of (part of) the mutant's LPS functionality.

Tailocin Gene Clusters of *P. putida* and *P. aeruginosa*: Located at Different Hot Spots, Carrying Similar Tail Cassettes but Equipped with Distinct Lysis and Regulatory Modules

The overall organization of the *P. putida* BW11M1 and RW10S2 tailocin gene clusters is similar to those of *P. aeruginosa* for R-type pyocin production (fig. 2). However, although their tail assembly modules exhibit extensive synteny, the lysis cassettes differ substantially. Although both species share homologous genes encoding a cytoplasmic membrane-permeabilizing holin (PtbB; 64% AA identity) and a peptidoglycan hydrolase (PtbR; 50% AA identity), positioned proximal and distal to the tail region, respectively, the *P. putida* systems encode different accessory proteins predicted to destabilize the cell envelope. The gene products PtbS and PtbT belong

to the same protein family as, respectively, Rz (an integral membrane protein; Pfam PF03245) and Rz1 (an outer membrane lipoprotein; Pfam PF06085), the spanins that are part of the phage λ lysis cassette (Catalão et al. 2013). The remarkable "Siamese twin" spanin gene organization, with the Rz1 coding region being embedded entirely within the Rz gene but transcribed in a different reading frame (+1), is conserved in both *P. putida* strains, as well as in *P. fluorescens* SF4c (Fischer et al. 2012). However, in the latter strain the "hidden" *rz1* homolog was not annotated due to the overlap by the open reading frame specifying the Rz-like gene product (Fischer et al. 2012). Another deviation from the prototypical R-type pyocin gene organization is the absence of equivalents of the *P. aeruginosa* regulatory genes *prtN* and *ptrB*, located downstream and upstream of *prtR*, respectively (fig. 2). A counterpart of the *prtR* gene (*ptbA*) is present but, unlike *prtR*, it is transcribed from the same DNA strand as the tail and lysis genes. Notably, PtbA shares rather low AA identity (38%) with the *P. aeruginosa* repressor protein. Yet another striking difference with the *P. aeruginosa* system concerns the genomic position of the *P. putida* BW11M1 and RW10S2 tailocin gene clusters that are found between the stress response genes *mutS* and *cinA–recA–recX*. Partial sequence analysis of the genomic regions upstream of *mutS* and *cinA* in *P. fluorescens* SF4c revealed the same location (Fischer et al. 2012), whereas R-type pyocin genes are consistently positioned between the AA anabolic genes *trpE* and *trpG*.

Abundance of R-Type Tailocins in Rhizospheric Pseudomonads

To explore the occurrence of R-type tailocins, we searched *Pseudomonas* genomes for regions carrying phage tail-like genes homologous to those identified in *P. putida* BW11M1/RW10S2 and exhibiting organizational similarity. This analysis revealed several tailocin-type gene clusters (~47), consistently sandwiched between *mutS* and *cinA* (supplementary table S3, Supplementary Material online). Their diversity is illustrated by the fact that only two of these have an identical nucleotide sequence: The strains *Pseudomonas simiae* WCS417 and *Pseudomonas* sp. R81 were both isolated from wheat roots but originate from remote agricultural areas (the Netherlands and India, respectively). In addition, near identity (99.5%) is displayed between the corresponding genomic regions in the biocontrol strains *P. fluorescens* A506, originating from pear phyllosphere (USA), and *P. fluorescens* WCS374, retrieved from potato rhizosphere (the Netherlands). Apparently, occurrence of strains with a particular tailocin element is not geographically restricted.

This search further revealed that the *P. aeruginosa*-type of pyocin R gene cluster is not only confined to this pathogenic species but also occurs in several environmental isolates degrading xenobiotics or plant-derived metabolites: For example, *Pseudomonas knackmussii* B13 (Miyazaki et al. 2014), *Pseudomonas nitroreducens* HBP1 (Garcia et al. 2014), *P. nitroreducens* TX1 (Huang et al. 2014), and *Pseudomonas* sp. M1 (Soares-Castro and Santos 2013). A pyocin cluster nearly identical to the latter, except for the tail fiber region, is present in two other strains, *Pseudomonas* sp. AAC and PI1.

Spanin-Like Proteins Are Part of the Lytic Cassettes of Most *P. putida* and *P. fluorescens* Tailocins

The BW11M1 and RW10S2 PtbB proteins, together with the large majority of the pseudomonad tailocin holins, belong to the same TC family (http://www.tcdb.org) (Saier and Reddy 2015) as the *P. aeruginosa* pyocin R holins (TC−1.E.20) and are not related to the P2 type (TC−1.E.3) or ΦCTX type (TC−1.E.56). Apart from a short, highly charged carboxy-terminal stretch (<20 AA), the PtbB sequences are strongly conserved among pseudomonads (supplementary file S1*A*, Supplementary Material online). Induced expression of the *P. fluorescens* Q8r1-96 PtbB homolog in *E. coli* cells engendered rapid cell lysis (Mavrodi et al. 2009).

The predicted BW11M1 and RW10S2 peptidoglycan hydrolases (PtbRs) lack a detectable secretory signal peptide and presumably act as canonical endolysins on peptidoglycan exposed by the action of the respective holins (Catalão et al. 2013). This type of endolysin appears to be common to the pseudomonad tailocins and the lytic capacity of the *P. fluorescens* Q8r1-96 PtbR homolog was demonstrated previously (Mavrodi et al. 2009). Belonging to the glycoside hydrolase family 19 (Pfam PF00182; CAZY-GH19; http://www.cazy.org), these enzymes are different from the lysozyme deployed by P2 (glycoside hydrolase family 24; PF00959) and the peptidoglycan-binding endolysin of ΦCTX (carrying domains PF01471 and PF11860). Remarkably, among characterized *Caudovirales* phages the most similar homologs are not found among *Myoviridae* members, with only less than 40% AA identity to the endolysin of enterobacteriohage 4MG (Kim et al. 2014). Significantly better matches are detected for a strain of the *Podoviridae* lysing *P. aeruginosa* (Jeon et al. 2012) and a strain of the *Siphoviridae* infecting *P. syringae* pv. *actinidiae* (Di Lallo et al. 2014) (supplementary file S2, Supplementary Material online).

The Rz/Rz1 module is widespread among phages infecting Gram-negative bacteria (Young 2014) and is also part of most of the pseudomonad tailocins. However, it is absent from the gene clusters of *P. aeruginosa* and a few other isolates (*P. fluorescens* strains A506 and FH5; *Pseudomonas* sp. strains CF150, CFT9, WCS347, and WCS417). The *rz/rz1* gene pair is equally absent from ΦCTX that carries partially overlapping spanin genes (Summer et al. 2007). Close to their carboxy-terminal end, the Rz proteins of BW11M1 and RW10S2 carry a cysteine residue that is conserved in the other inspected pseudomonad tailocins (supplementary file S1*B*, Supplementary Material online). The smaller Rz1 proteins have, in addition to the characteristic amino-terminal cysteine

required for lipoprotein formation, two other cysteines that are perfectly conserved among these tailocins (supplementary file S1C, Supplementary Material online). This suggests that disulphide bond formation could be important for the function of these spanins (Berry et al. 2012, 2013).

Dedicated Tailocin Regulatory Proteins Differ between *P. aeruginosa* and Other Pseudomonads

The regulatory proteins of pseudomonad tailocins, PrtR (*P. aeruginosa*) and PtbA (mainly *P. putida* and *P. fluorescens* groups) appear to be specific for these bacteriocins as no close homologs were identified in (pro)phages. The best matches to PtbAs (~55% AA identity) and PrtRs (~42% identity) are shown by, respectively, lambdoid prophage 06 of *P. protegens* Pf-5 (Mavrodi et al. 2009) and *P. aeruginosa* temperate phage PAN70 (Rangel et al. 2013). The PrtR and PtbA sequences show strong sequence conservation within each subfamily (>80% AA sequence identity) but there is only low similarity between members from the respective subfamilies (<40% AA sequence identity). Although in *P. aeruginosa* PrtR represses *prtN* expression, no homolog of the latter is found in combination with *ptbA*.

A Bacteriocin Cargo Embedded in the R Tailocin Gene Cluster of *P. putida* BW11M1

Comparison of the tailocin gene clusters of *P. putida* BW11M1 and *P. putida* RW10S2 revealed the presence of the BW11M1 structural gene encoding the lectin-like bacteriocin LlpA (fig. 2). A second "cargo" gene located upstream of *llpA* encodes a homolog of bacteriophage Mu translational regulator Com (Hattman 1999). This gene organization is conserved in *Pseudomonas mosselii* SJ10. Also elsewhere in the tailocin clusters of *P. fluorescens* DSM 8569 and F113, *Pseudomonas parafulva* CRS01-1, *P. putida* RW10S2, and *Pseudomonas* sp. GM67, a *com* homolog is apparently linked to a (different) cargo gene of unknown function (fig. 3). Rather unexpectedly, we detected LlpA in the MS-analyzed purified R_{BW11M1} tailocin sample (supplementary table S2, Supplementary Material online). LlpA is readily detectable in the culture supernatant of BW11M1 stationary phase cells but its production can be significantly enhanced by UV-induced DNA damage (Parret et al. 2003). Apparently, when LlpA and the tailocin are coexpressed, (part of) the lectin remains associated with the particles. Also in the RW10S2 tailocin preparation, the *com*-linked cargo protein was detected (fig. 2).

Although the tail region of the tailocins in the various strains is well conserved, significant sequence variation is apparent near either end of it, but in particular in the regions flanking the repressor and holin genes (fig. 3). Most of the predicted gene products are hypothetical proteins of unknown functions, but to some a tentative function can be assigned: A peptidoglycan peptidase (Lee et al. 2013) and a YafO-like protein synthesis inhibitor (Zhang et al. 2009) in *P. fluorescens* SS101, a putative Zeta family toxin inhibiting peptidoglycan synthesis in *P. fluorescens* strains BBc6R8 and ATCC 17400 (Mutschler and Meinhart 2011), a putative LPS-modifying acyltransferase in *P. putida* UASWS0946, and a potential UV radiation-protective RulA–RulB module in *P. putida* BW11M1 (Sundin et al. 2000). *Pseudomonas putida* MTCC 5279 carries tailocin-associated metabolic

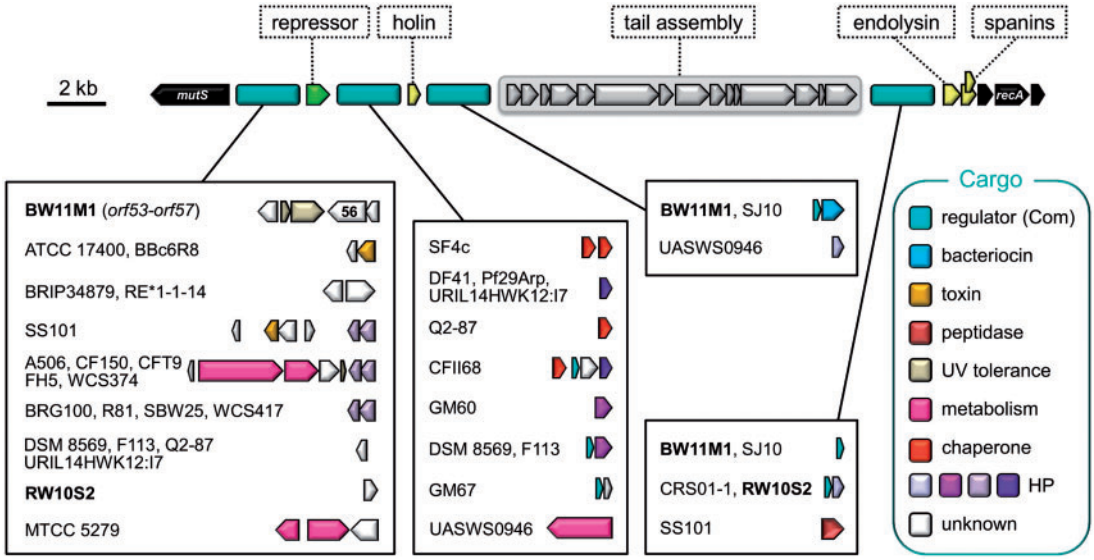

Fig. 3.—General organization of *Pseudomonas* R tailocin clusters with insertion sites of cargo genes (teal). Arrows illustrate coding regions and are colored as in figure 2, except for the tail assembly module (in gray), and their respective functions are shown in dotted boxes. Cargo genes inserted at one of the four sites, together with their *Pseudomonas* strain of origin, are shown in separate boxes. The (predicted) function of the cargo gene products is specified by a color legend. Homologous genes are shown in the same color.

genes, encoding an oxygenase, an AA transporter, and a linked LysR family regulator. A larger cargo region with presumptive metabolic capacity (including carboxylase, 2-hydroxyacid dehydrogenase, and methyltransferase genes) is conserved in five strains.

Distinct Tailocin Clades Pointing to Different (Pro)phage Ancestries

Inspection of *Pseudomonas* genomes for regions bearing similarity to the *P. putida* BW11M1/RW10S2 tailocin genetic backbones also revealed many putative prophage clusters typically located at sites other than the *mutS–cinA* intergenic region (supplementary table S3, Supplementary Material online). To scrutinize the evolutionary relationship of the pseudomonad tailocins with these prophages, as well as with related sequenced phages, we focused on their most conserved proteins: Ptb proteins equivalent to the phage P2 proteins building the tail spike (PtbD, GpV), tail sheath (PtbJ, GpFI), tail tube (PtbK, GpFII), baseplate hub (PtbQ, GpD), and baseplate (PtbE–PtbF, GpW–GpJ). The Gp nomenclature refers to P2 proteins, as described by Sarris et al. (2014). In addition, corresponding homologs of the P2-related γ-proteobacterial tailocins, maltocin from *Stenotrophomonas maltophilia* (Liu et al. 2013) and photorhabdicin from *Photorhabdus luminescens* (Gaudriault et al. 2004), are included. The latter is closely related to xenorhabdicin from *Xenorhabdus bovienii* (Morales-Soto et al. 2012). Their gene organization and sequences differ substantially from the morphologically related carotovoricin produced by *Pectobacterium carotovorum* (*Erwinia carotovora*) which is therefore not included in this comparison (Yamada et al. 2006).

The respective phylogenetic trees inferred from multiple sequence alignments of these structural proteins display a similar overall topology, with pseudomonad sequences being distributed across three main clusters, designated Rp1 through Rp3 (with Rp referring to R-type pseudomonad phage-like bacteriocin). These clusters are delineated in a representative simplified phylogenetic tree for the PtbK tail tube protein (fig. 4; full version in supplementary file S3*A*, Supplementary Material online). The related *P. putida* BW11M1/RW10S2 sequences (Rp2) and the *P. aeruginosa*-like subset (Rp1) are located on separate branches of the major clade, that is further populated by a number of other tailocin proteins and most prophage proteins. For the other conserved proteins, the derived trees are shown in supplementary file S3*B* (tail spike protein PtbD), S3*C* (baseplate protein PtbE), S3*D* (baseplate protein PtbF), S3*E* (tail sheath protein PtbJ), and S3*F* (baseplate hub protein PtbQ), Supplementary Material online.

The *P. aeruginosa*-like subset (Rp1) appears to be related to the *P. aeruginosa* phage PS17, based on phylogeny of the tail tube and tail sheath proteins (PtbK, supplementary file S3*A*, Supplementary Material online; PtbJ, supplementary file S3*E*, Supplementary Material online). Although no other sequence information is available for this phage (Shinomiya and Ina 1989), the phylogenetic clustering is in line with the observations that PS17 and R pyocins are closely related (Kageyama et al. 1979), even allowing functional exchange of tail components (Shinomiya 1984; Williams et al. 2008) and enabling pyocin-based modeling of the phage tail tube structure (Ge et al. 2015). The Rp2 branch includes the putative tail tube protein encoded by the BW11M1 prophage occupying the DNA region between the apparent cargo genes flanking *ptbA* (*orf53–orf57*; fig. 5) and *mutS*. MS analysis of the BW11M1 tailocin did not reveal trypic peptides potentially specified by this prophage cluster (supplementary table S2, Supplementary Material online). This type of prophage is absent from the RW10S1 and RW10S2 genomes but related prophages with syntenic tail regions are present in several other pseudomonads (supplementary table S3, Supplementary Material online). Based on differences in the respective capsid-encoding regions, two additional subtypes can be distinguished. The organization of these Rp1/Rp2-related prophages is illustrated in figure 5. For the *P. putida* KT2440 representative, carrying a siphoviral head (prophage 2, corresponding to the cluster encoding PP3026–PP3066; Wu et al. 2011), no physiological conditions could be detected that triggered its excision (Martínez-García et al. 2015).

The majority of the R tailocins constitutes a second, quite distant clade (Rp3) to which no proteins originating from pseudomonad (pro)phages were assigned. This implies that the structurally related tailocin/prophage pairs, as co-occurring in *P. fluorescens* strains A506, F113, Q2-87, and Q8r1-96 and in *Pseudomonas veronii* 1YdBTEX2, are probably of different origins. The phylogenetic distance of Rp3 from the Rp1/Rp2 clade can be illustrated by the marginal sequence identity between the main tail structural proteins: The *P. fluorescens* SF4c (Rp3) tube and sheath proteins share only between 19% and 24% AA identity with the respective protomers of *P. aeruginosa* PAO1 (Rp1) and *P. putida* BW11M1 (Rp2). The closest protein neighbors for the large group of Rp3 tailocins are not found among characterized pseudomonad phages but in the tail structural proteins of *Vibrio parahaemolyticus* phage VP882 (Lan et al. 2009) and *Halomonas aquamarina* phage ΦHAP-1 (Mobberley et al. 2008) (fig. 5). With the *P. fluorescens* SF4c tailocin sheath and tube proteins, these phages share 36–39% and 55–57% identity, respectively. VP882 and ΦHAP-1 are temperate phages with a linear plasmid-like genome, belonging to the *Hapunalikevirus* genus within the *Myoviridae* (http://viralzone.expasy.org/). A few of the identified pseudomonad prophages exhibit structural protein homology and pronounced synteny (illustrated for *P. fluorescens* A506; fig. 5) with P2 and ΦCTX, both members of the genus *P2likevirus* of *Myoviridae* (Nakayama et al. 1999; Alber et al. 2002). Although photorhabdicin bears prominent phylogenetic relatedness with these phages (fig. 4), this is not the case for any of the pseudomonad tailocins. Maltocin, on the

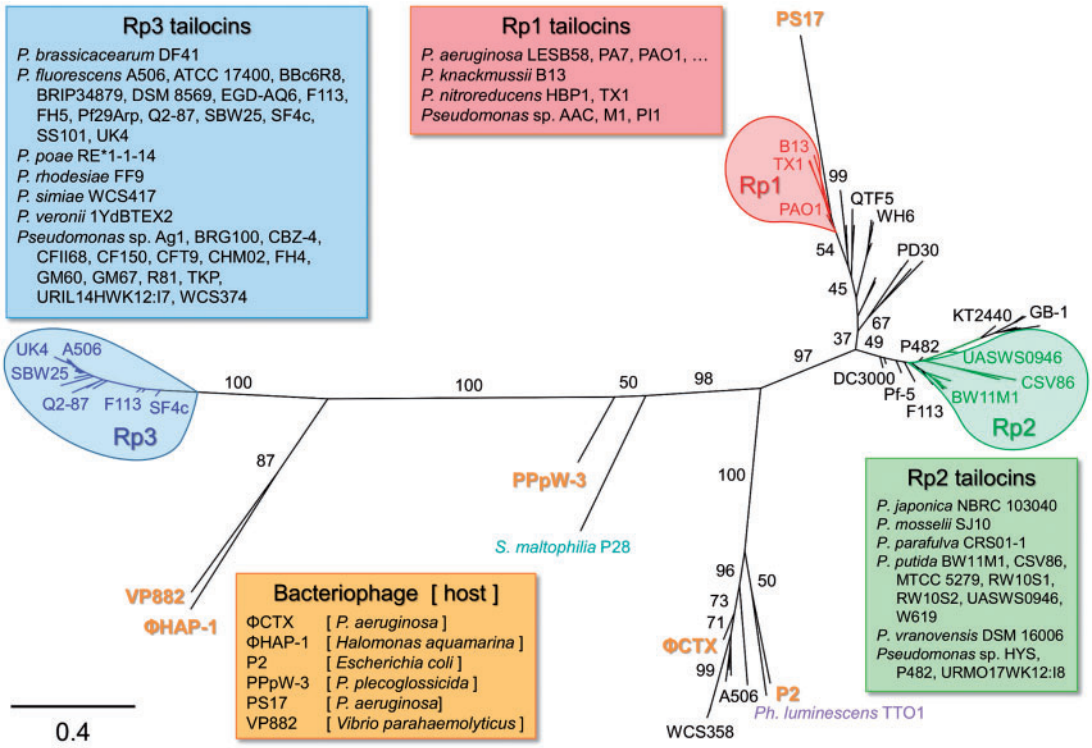

Fig. 4.—Phylogenetic analysis of tail tube proteins in *Pseudomonas* R tailocins. The unrooted maximum-likelihood tree is derived from a multiple AA sequence alignment of PtbK proteins with homologs from characterized phages, predicted pseudomonad prophages, and γ-proteobacterial R tailocin-like antibacterial particles. Three clusters encompassing tail tube proteins from the Rp1 group (red), Rp2 group (green), and Rp3 group (blue) are highlighted. Tail tube proteins from phages (orange), prophages (black), maltocin (teal), and photorhabdicin (purple) are marked in distinct colors. For reasons of visibility, only selected strain names are shown at the corresponding tailocin and prophage branches (fully annotated tree in supplementary file S3*A*, Supplementary Material online); all strains in the tree are listed in boxes with group-corresponding colors (the origin of the strains is specified in supplementary table S3, Supplementary Material online). The scale bar represents 0.4 substitutions per site. Bootstrap values (percentages of 1,000 replicates) are shown at the major branches. Other tailocin and (pro)phage structural proteins display similar tree topologies: Tail spike protein PtbD, baseplate protein PtbE, baseplate protein PtbF, tail sheath protein PtbJ, and baseplate hub protein PtbQ (supplementary file S1*B–F*, Supplementary Material online, respectively).

other hand, appears to share a common ancestry with a *Pseudomonas plecoglossicida* phage, PPpW-3 (Kawato et al. 2015; fig. 5).

The similarity between pseudomonad tailocins and related prophages is not confined to the conserved structural proteins but extends to the associated lytic modules of most of these prophages. These cassettes include holins belonging to the same TC−1.E.20 family. However, the tailocin- and prophage-derived proteins tend to cluster on separate branches, even for representatives encoded by a single strain, as is the case for *P. putida* BW11M1. This indicates that the tailocin-type (PtbB) and prophage holins evolved separately (data not shown). A similar conclusion can be drawn for the tailocin-type of endolysin (PtbR) and the PtbR-like prophage enzymes (supplementary file S2, Supplementary Material online). Likewise, although the spanin-encoding segment is typically poorly annotated, careful inspection reveals that the *rz/rz1* spanin gene architecture appears to be common to the tailocin-related prophages.

Tail Fiber Proteins: Highly Diversified Determinants of Target Strain Specificity

The tail fiber protein (TfpH) of R pyocins is the major specificity determinant for killing *P. aeruginosa* strains (Williams et al. 2008). The equivalent PtbH proteins share an amino-terminal domain of unknown function (~150–160 AA, DUF3751; Pfam PF12571), followed by a polypeptide sequence that is quite variable in sequence and length. The PtbH proteins can be subdivided into three main groups. A first type of putative tail fiber protein is essentially composed of only the conserved DUF3751 domain ("a-type" tail fiber; supplementary table S3, Supplementary Material online). This "short" DUF3751 variant, present in a subset of tailocins, and prophages, is also found in the nonpseudomonad phages VP882 and ΦHAP-1 (fig. 5). A second group, including BW11M1 PtbH (815 AA), bears a much longer carboxy-terminal domain ("b-type" tail fiber protein; supplementary table S3, Supplementary Material online). A similar architecture is also present in pseudomonad homologs from several other tailocin clusters, many

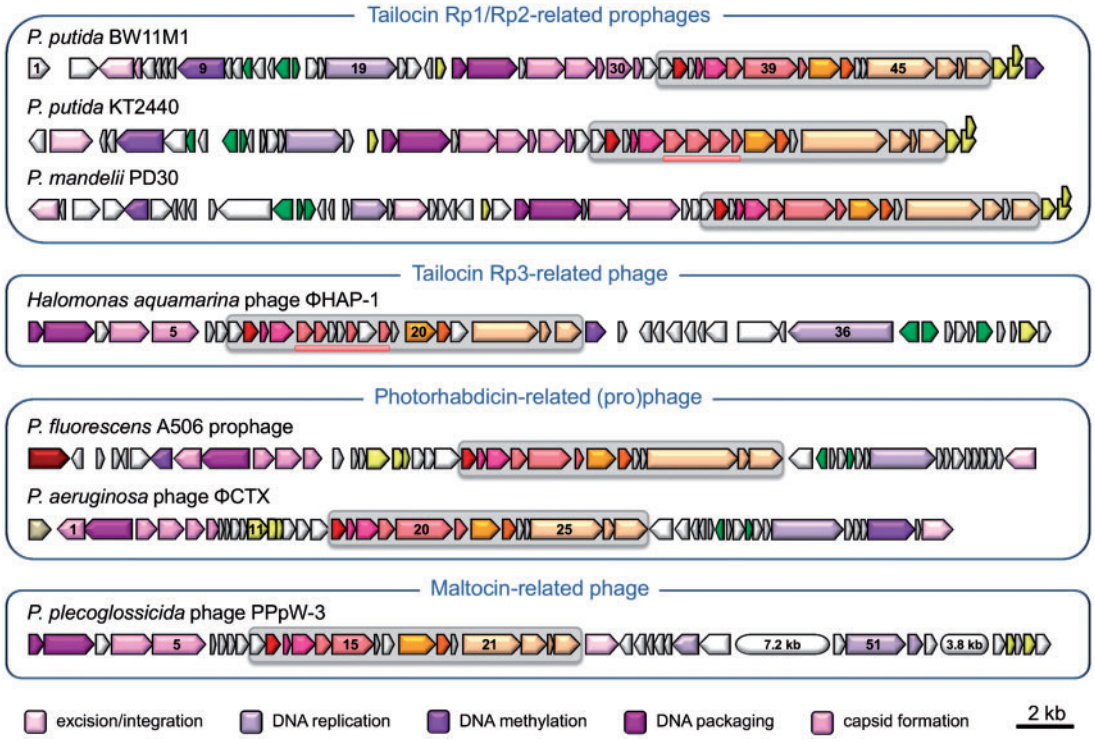

Fig. 5.—Schematic overview of the genetic organization of representative tailocin-related phages and prophages. The phage genomes and prophage regions are grouped in boxes labeled according to the phylogenetic clustering shown in figure 4. Arrows represent coding regions and are colored according to their predicted function as specified in figure 2. Additional functions of (pro)phage-specific genes are defined (see enclosed color legend). The cassettes encoding the (pro)phage tail regions are delineated with gray boxes. Tail fiber regions with a short tail fiber gene (encoding an a-type DUF3751 protein) are marked with a bar within these boxes. Prophages related to ΦCTX as present in *P. fluorescens* A506 are also found *P. fluorescens* Q2-87 and Q8r1-96, *P. protegens* CHA0, *P. putida* HB3267, *P. mendocina* NK-01, and *Pseudomonas* sp. WCS358. The scale bar corresponds to a 2-kb DNA region.

presumptive prophages, and phages such as ΦCTX and PS17. In a third set of tail fibers (c-type), DUF3751 is accompanied by an additional domain of unknown function (Pfam PF07484), originally identified in the tail fiber protein Gp12 of bacteriophage T4 (Makhov et al. 1993). Although this fiber protein type is very abundant among pseudomonad R tailocins, including those of *P. fluorescens* strains SF4c (998 AA) and *P. putida* RW10S2 (748 AA), it is only occurring in a few of the retrieved prophages (supplementary table S3, Supplementary Material online).

Due to the huge sequence divergence and length differences of the carboxy-terminal regions in TfpH/PtbH proteins, only their amino-terminal part with the DUF3751 domain can be meaningfully aligned. The phylogenetic tree inferred from this alignment displays a dichotomous topology reminiscent of those of the much more conserved tail structural proteins, albeit with additional subclusters and more dispersed branches (fig. 6). One major cluster of a-type DUF3751 proteins encompasses those present in about half of Rp3-type tailocins (17 strains), being clearly related to the *Vibrio* and *Halomonas* phage-associated proteins. The b-type DUF3751-containing pseudomonad proteins are dispersed across the phylogenetic tree and represent members of the Rp1 and Rp2 tailocins, along with a second set of Rp3-type tailocins (16 strains). The DUF3751 domain of most *P. aeruginosa* strains bears close similarity with the corresponding ΦCTX and PS17 domains. However, a second P2-related type is present in the atypical strain *P. aeruginosa* PA7 (Roy et al. 2010) and is shared by the *P. knackmussii*/*P. nitroreducens* group of strains.

TfpH and its cognate chaperone (encoded by the gene downstream of *tfpH*), the tail tape measure protein (encoded by the *ptm* gene located further downstream) that controls the final length of the tail tube (Leiman and Shneider 2012), are specified by the least conserved DNA stretch (nucleotide sequence and coding length) in *P. aeruginosa* R-type pyocin clusters. The equivalent tail tape measure protein PtbN of *P. putida* BW11M1 and RW10S2 tailocins differs substantially in length (762 vs. 676 AA) and shares only marginal AA sequence identity (21%). This reflects the poor sequence conservation and broad size range (354–963 AA) within the TfpH/PtbN family. Although the size of tailocin PtbN homologs is typically well below 1,000 AA (average 628 AA), the equivalent pseudomonad prophage proteins are significantly longer (780–1,315 AA; average 980 AA, P value < 2.2 e-16; fig. 6). This would suggest that the tailocin tubes are generally

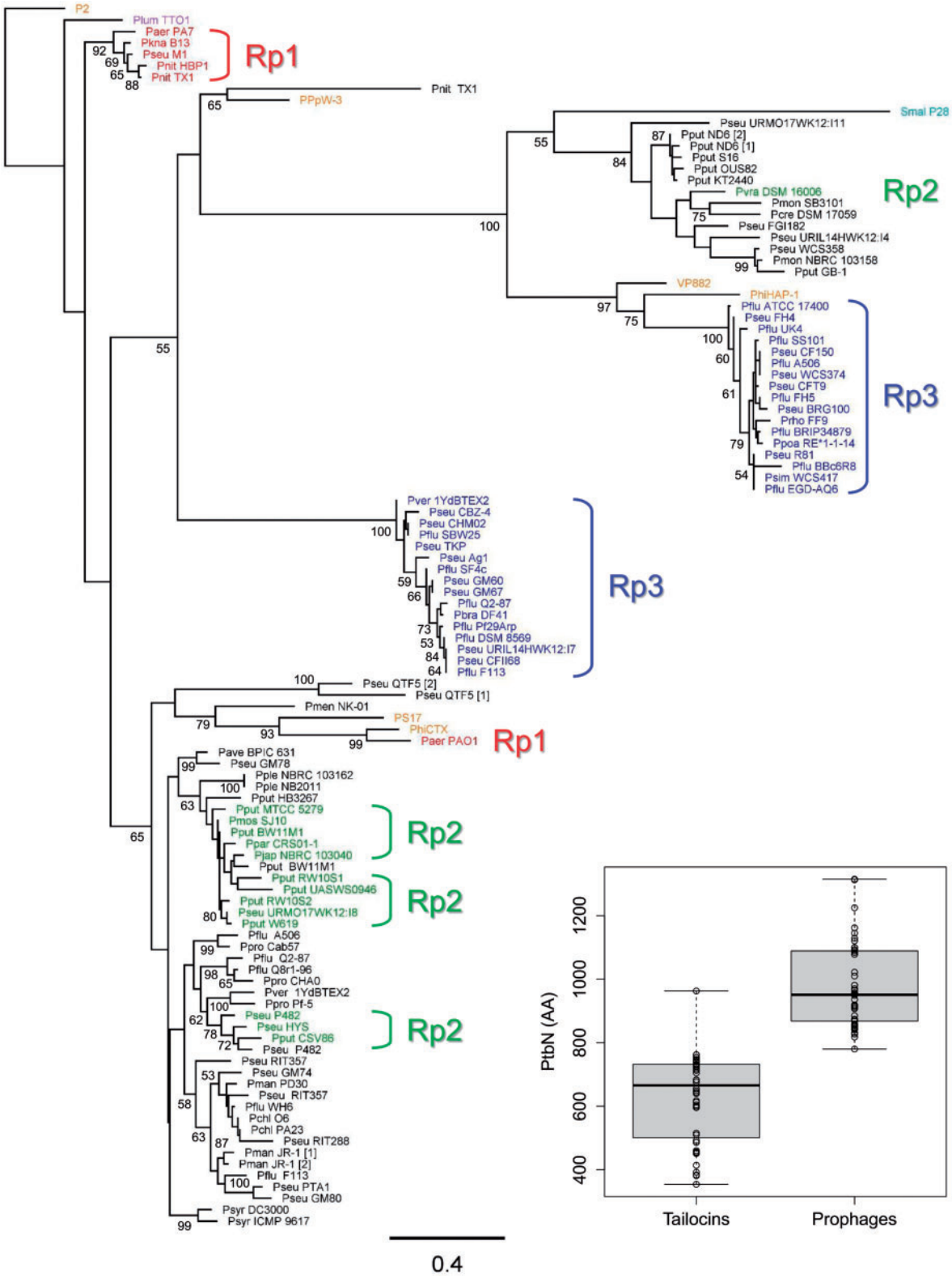

FIG. 6.—Phylogenetic analysis of tail fiber proteins in *Pseudomonas* R tailocins. The maximum-likelihood tree was derived from a multiple AA sequence alignment of the amino-terminal DUF3751 domains in PtbH proteins and in homologs from characterized phages (with P2 sequence as root), predicted pseudomonad prophages, and γ-proteobacterial R tailocin-like antibacterial particles. The same colors were used as for the PtbK tree (fig. 4). The scale bar represents 0.4 substitutions per site. Bootstrap values (percentages of 1,000 replicates) are shown at the major branches. The size distributions (in amino acids) of phage tail tape measure proteins of R tailocins (PtbN) and homologs from *Pseudomonas* prophages are shown in box plots.

shorter than those of structurally related pseudomonad (pro)phages.

Even between tailocin gene clusters that overall share a very high level of nucleotide sequence identity, the similarity in the DNA regions encoding tail fiber/chaperone/tape measure proteins can drop substantially. This can be illustrated by the extensive synteny between the gene clusters of *P. putida* BW11M1 and *P. mosselii* SJ10 that even spans their cargo genes (including a 99% identical copy of the encoded bacteriocin LlpA), and yet the nucleotide sequence identity between their *ptbH–ptbI–ptbN* regions is only about 50% (compared with >90% for the remaining parts).

General Discussion

Phage tail-derived elements integrated in bacterial genomes mediate diverse interactions with other organisms. Afp (antifeeding prophage of *Serratia entomophila*) and PVC (*Photorhabdus* virulence cassette) are similar delivery vehicles that inject toxins into insect hosts (Hurst et al. 2004; Yang et al. 2006). Ordered arrays of MAC (metamorphosis-associated contractile structure) produced by biofilm-producing *Pseudoalteromonas luteoviolaceae* trigger metamorphosis in larvae of a marine invertebrate upon contact with the sessile bacteria (Shikuma et al. 2014). These systems share some features with the Type VI secretion machinery that delivers inhibitor or effector molecules to fellow prokaryotes or eukaryotic host cells (Durand et al. 2014; Russell et al. 2014) but their genetic make-up and contractile tail structure hint to an evolutionary relatedness to R-type pyocins (Heymann et al. 2013; Sarris et al. 2014). Most strains of the opportunistic human pathogen *P. aeruginosa* have the capacity to release HMW complexes (R- and/or F-type pyocins) with intraspecies bacteriocin activity (Ghequire and De Mot 2014). Early studies on the morphology of these killing particles revealed striking similarity with phage tails, which was further substantiated upon identification of the corresponding gene clusters (Nakayama et al. 2000). Similar phage tail-like bacteriocins have been described for several other γ-proteobacterial genera (Coetzee et al. 1968; Thaler et al. 1995; Strauch et al. 2001; Jabrane et al. 2002; Gaudriault et al. 2004; Smarda and Benada 2005; Yamada et al. 2006) and some Firmicutes (Zink et al. 1995; Gebhart et al. 2012).

Following functional and genetic characterization of R-type tailocins in two *P. putida* strains, comparative analysis of pseudomonad genomes revealed that this type of tailocin and related prophage clusters are equally abundant in species other than *P. aeruginosa*. The phylogeny of the tailocin structural proteins in pseudomonads reveals an unexpected dichotomy with two main clades: One including the tailocins from the *P. putida* strains, related to those of *P. aeruginosa*, and a second distant clade represented mainly by *P. fluorescens* strains. For neither of these groups, particularly close similarity is apparent to the corresponding tail proteins of the HMW bacteriocins from other γ-proteobacteria. In addition, our comparative analysis advocates for a reappraisal of the current view, stemming from the work of Nakayama et al. (1999, 2000) about the shared ancestry of R-type pyocins with the P2-related pseudomonad phage ΦCTX. Although the P2/ΦCTX-relatedness is pronounced for photorhabdicin, the *P. aeruginosa* R pyocins appear more closely related to *P. aeruginosa* phage PS17. Production of this type of R pyocin is apparently not confined to the pathogen *P. aeruginosa* as quite similar gene clusters are found at the same genomic location (*trpE–trpG* intergenic region) in the genomes of other species such as *P. knackmussii* and *P. nitroreducens*. A large number of pseudomonad prophages encode structural proteins with homology to the tailocin sequences from the *P. aeruginosa*/*P. putida* mixed clade. For the *P. fluorescens* group of tailocins, on the other hand, no such close prophage relatives can be pinpointed. Their nearest structural protein neighbors are found in prophages that are maintained as linear plasmid-like entities in γ-proteobacterial hosts (*Halomonas*, *Vibrio*), which suggests a different evolutionary origin and route of acquisition compared with the tailocins of the *P. aeruginosa* and *P. putida* complexes. Based on these observations, we propose a new phylogeny-based classification of these particles in pseudomonads (fig. 4): Tailocins Rp1, Rp2, and Rp3, with "R" referring to the R-type, "p" referring to pseudomonads, and the number specifying the "species complex" of origin (with *P. aeruginosa*, *P. putida*, and *P. fluorescens*, respectively, as main representative species). Rp1 tailocins consistently differ from Rp2 and Rp3 tailocins with respect to genomic location, regulatory module, and lysis cassette. Possibly, adaptation to specific niches, for instance, by a pathogen such as *P. aeruginosa* to a human host environment or a saprophyte such as *P. fluorescens* or *P. putida* to a plant root environment, has driven such differences in tailocin domestication (Touchon et al. 2014).

Compared with the limited number of different tail fiber proteins found among *P. aeruginosa* R-type pyocins, the sequences of these tailocin proteins have diverged extensively among other pseudomonad species. Based on domain architecture, the subtypes a (short), b ("long" with only DUF3751), and c (long with DUF3751 and PF07484) are distinguished, which can be further differentiated by AA sequence and length (supplementary table S3, Supplementary Material online). This can be useful to subdivide the Rp types: For instance, *P. putida* BW11M1 and RW10S2 produce Rp2b and Rp2c tailocins, respectively, whereas *Pseudomonas vranovensis* DSM 16006 is designated a potential Rp2a producer; tailocins from *P. fluorescens* A506, F113, and SF4c would be typed Rp3a, Rp3b, and Rp3c, respectively; *P. aeruginosa*, *P. knackmussii*, and *P. nitroreducens* share the same type of tailocin (Rp1b). The huge diversity among tail fiber proteins suggests that a particular tailocin will probably be able to kill only a confined subset of other pseudomonad strains and

hence typically display a narrow spectrum, as observed for the HMW bacteriocins from *P. putida* BW11M1 and RW10S2.

Recently, a fourth type of R-type tailocin (Rp4), syringacin of the phytopathogen *P. syringae* pv. *syringae* B728a, was functionally characterized. Based on comparative analysis of baseplate and tail sheath proteins, this tailocin is only distantly related to the Rp1–Rp2–Rp3 clusters, in line with its striking genomic synteny to SfV (Hockett et al. 2015). SfV is a member of a group of temperate serotype-converting Mu-like *Shigella flexneri* phages within the *Myoviridae* (Grose and Casjens 2014). Hence, this study lends further support to our differential ancestry hypothesis for pseudomonad tailocins. Despite an apparently quite different route of tail gene domestication, the Rp4 tailocin has adopted a very similar lysis cassette, including the "Russian doll" organization of spanin genes (although *rz1* is not yet annotated in strain B728a). *Pseudomonas syringae* houses the R-type syringacin cluster at the same genomic position as where *P. aeruginosa* harbors its tailocins (between *trpE* and *trpG*). It also carries an Rp1-type of regulatory module (*rtsB–rtsA*, equivalent of *prtR–prtN*) but lacks the accessory *ptrB* gene that coordinates pyocin production and expression of Type III secretion in *P. aeruginosa* (Wu and Jin 2005). However, in strains of other species (such as *Pseudomonas brassicacearum* NFM421, *P. fluorescens* Q8r1-96, *Pseudomonas mandelii* JR-1, and *P. protegens* Pf-5) only a PtbA-like regulatory gene is present in their Rp4-like cluster that is integrated between *mutS* and *cinA*, features which are typically associated with the Rp2 and Rp3 tailocins.

In several *P. aeruginosa* strains the Rp1 gene cluster is linked to a F-type tailocin, both relying for expression and release on a common set of regulatory and lysis genes (Ghequire and De Mot 2014). Inspection of genomic regions with one of the three other R-type tailocins has revealed that, in addition to clusters encoding a single tailocin, multiple combinations of them exist (some including a tailocin of the F-type) in which two or three tailocins are neatly fused between the regulatory and lytic genes, suggesting a capacity for concomitant production of two or three different tailocins (Ghequire and De Mot 2015). The presence in the *mutS–cinA* intergenic region of a prophage adjacent to a tailocin, each with their own regulatory and lytic modules, as observed in *P. putida* BW11M1, apparently also occurred in some other strains. In these combinations tail regions of prophage and tailocin(s) are not necessarily of the same type, which indicates that these mobile elements can be co-opted independently.

Several plant-associated pseudomonad strains have recruited additional genes to the external regions of the tailocin gene clusters, leaving the tail-assembly module intact. These acquired genes may contribute to the ecological fitness and competitiveness of their carrier bacteria. Such function in interference competition is likely for the Rp2-embedded lectin-like bacteriocin genes of *P. putida* BW11M1. Apparently, one of two lectin-like bacteriocins (LlpA1; Parret et al. 2005) and a secreted chitinase (glycoside hydrolase family 18; PDB 4Q6T) are actually encoded by cargo genes of an Rp4-like tailocin cluster present in *P. protegens* Pf-5. The bacteriocin-within-tailocin configuration is equally present in the *P. fluorescens* Q8r1-96 genome, where this strain's colicin M-like lipid II-degrading bacteriocin (Barreteau et al. 2012) is also encoded by an Rp4-type tailocin cargo gene. Such Rp4-associated colicin M-like genes are found in other isolates as well (*P. syringae* 642 and *P. brassicacearum* NFM42). The Rp4 cargo gene *rtsE* of *P. syringae* B728a also encodes a putative glycoside hydrolase (family 5; Pfam PF00150). Our observation that some proteins encoded by cargo genes embedded within tailocin gene clusters may remain physically associated with mature tailocin particles requires further scrutiny to assess whether such hitchhiking is a more general phenomenon and is of biological relevance.

Supplementary Material

Supplementary files S1–S3 and tables S1–S3 are available at *Genome Biology and Evolution* online (http://www.gbe.oxfordjournals.org/).

Acknowledgments

This work was partially supported by the FNRS under grant "Grand equipement" no. 2877824 to R.W. M.G.K.G. is the recipient of an FWO postdoctoral fellowship (12M4615N). The authors thank Dr Sandra Van Puyvelde for technical assistance. They acknowledge the valuable comments provided by the reviewers.

Literature Cited

Alber J, Langewische FW, Adebayo AA, Lutz F. 2002. Organization and activation of the late promoters of ϕCTX, a cytotoxin-converting phage from *Pseudomonas aeruginosa*. Mol Genet Genomics. 267:38–44.

Barreteau H, et al. 2009. Human- and plant-pathogenic *Pseudomonas* species produce bacteriocins exhibiting colicin M-like hydrolase activity towards peptidoglycan precursors. J Bacteriol. 191:3657–3664.

Barreteau H, et al. 2012. Functional and structural characterization of PaeM, a colicin M-like bacteriocin produced by *Pseudomonas aeruginosa*. J Biol Chem. 287:37395–37405.

Baysse C, et al. 1999. Uptake of pyocin S3 occurs through the outer membrane ferripyoverdine type II receptor of *Pseudomonas aeruginosa*. J Bacteriol. 181:3849–3851.

Berry J, Rajaure M, Pang T, Young R. 2012. The spanin complex is essential for lambda lysis. J Bacteriol. 194:5667–5674.

Berry JD, Rajaure M, Young R. 2013. Spanin function requires subunit homodimerization through intermolecular disulfide bonds. Mol Microbiol. 88:35–47.

Braun V, Patzer SI. 2013. Intercellular communication by related bacterial protein toxins: colicins, contact-dependent inhibitors, and proteins exported by the type VI secretion system. FEMS Microbiol Lett. 345:13–21.

Catalão MJ, Gil F, Moniz-Pereira J, São-José C, Pimentel M. 2013. Diversity in bacterial lysis systems: bacteriophages show the way. FEMS Microbiol Rev. 37:554–571.

Coetzee HL, De Klerk HC, Coetzee JN, Smit JA. 1968. Bacteriophage-tail-like particles associated with intra-species killing of *Proteus vulgaris*. J Gen Virol. 2:29–36.

de los Santos PE, Parret AH, De Mot R. 2005. Stress-related *Pseudomonas* genes involved in production of bacteriocin LlpA. FEMS Microbiol Lett. 244:243–250.

Denayer S, Matthijs S, Cornelis P. 2007. Pyocin S2 (Sa) kills *Pseudomonas aeruginosa* strains via the FpvA type I ferripyoverdine receptor. J Bacteriol. 189:7663–7668.

Di Lallo G, et al. 2014. Isolation and partial characterization of bacteriophages infecting *Pseudomonas syringae* pv. *actinidiae*, causal agent of kiwifruit bacterial canker. J Basic Microbiol. 54:1210–1221.

Durand E, Cambillau C, Cascales E, Journet L. 2014. VgrG, Tae, Tle, and beyond: the versatile arsenal of Type VI secretion effectors. Trends Microbiol. 22:498–507.

El-Sayed AK, Hothersall J, Thomas CM. 2001. Quorum-sensing-dependent regulation of biosynthesis of the polyketide antibiotic mupirocin in *Pseudomonas fluorescens* NCIMB 10586. Microbiology 147:2127–2139.

Elfarash A, et al. 2014. Pore-forming pyocin S5 utilizes the FptA ferripyochelin receptor to kill *Pseudomonas aeruginosa*. Microbiology 160:261–269.

Elfarash A, Wei Q, Cornelis P. 2012. The soluble pyocins S2 and S4 from *Pseudomonas aeruginosa* bind to the same FpvAI receptor. Microbiologyopen 1:268–275.

Fischer S, et al. 2012. Characterization of a phage-like pyocin from the plant growth-promoting rhizobacterium *Pseudomonas fluorescens* SF4c. Microbiology 158:1493–1503.

Garcia JL, et al. 2014. Genome sequence of *Pseudomonas azelaica* HBP1, which catabolizes 2-hydroxybiphenyl fungicide. Genome Announc. 2:e01248–13.

Gaudriault S, et al. 2004. Identification of a P2-related prophage remnant locus of *Photorhabdus luminescens* encoding an R-type phage tail-like particle. FEMS Microbiol Lett. 233:223–231.

Ge P, et al. 2015. Atomic structures of a bactericidal contractile nanotube in its pre- and postcontraction states. Nat Struct Mol Biol. 22:377–382.

Gebhart D, et al. 2012. Novel high-molecular-weight, R-type bacteriocins of *Clostridium difficile*. J Bacteriol. 194:6240–6247.

Geels FP, Schippers B. 1983. Selection of antagonistic fluorescent *Pseudomonas* spp. and their root colonization and persistence following treatment of seed potatoes. J Phytopathol. 108:193–206.

Ghequire MG, De Mot R. 2014. Ribosomally encoded antibacterial proteins and peptides from *Pseudomonas*. FEMS Microbiol Rev. 38:523–568.

Ghequire MG, De Mot R. 2015. The tailocin tale: peeling off phage tails. Trends Microbiol. doi: 10.1016/j.tim.2015.07.011

Ghequire MG, et al. 2013. Structural determinants for activity and specificity of the bacterial toxin LlpA. PLoS Pathog. 9:e1003199.

Ghequire MG, et al. 2014. O serotype-independent susceptibility of *Pseudomonas aeruginosa* to lectin-like pyocins. Microbiologyopen 3:875–884.

Ghequire MG, Li W, Proost P, Loris R, De Mot R. 2012. Plant lectin-like antibacterial proteins from phytopathogens *Pseudomonas syringae* and *Xanthomonas citri*. Environ Microbiol Rep. 4:373–380.

Green MR, Sambrook J. 2012. Molecular cloning: a laboratory manual. New York: Cold Spring Harbor.

Grinter R, Roszak AW, Cogdell RJ, Milner JJ, Walker D. 2012. The crystal structure of the lipid II-degrading bacteriocin syringacin M suggests unexpected evolutionary relationships between colicin M-like bacteriocins. J Biol Chem. 287:38876–38888.

Grose JH, Casjens SR. 2014. Understanding the enormous diversity of bacteriophages: the tailed phages that infect the bacterial family *Enterobacteriaceae*. Virology 468–470:421–443.

Guindon S, Gascuel O. 2003. A simple, fast, and accurate algorithm to estimate large phylogenies by maximum likelihood. Syst Biol. 52:696–704.

Hattman S. 1999. Unusual transcriptional and translational regulation of the bacteriophage Mu *mom* operon. Pharmacol Ther. 84:367–388.

Hayes CS, Aoki SK, Low DA. 2010. Bacterial contact-dependent delivery systems. Annu Rev Genet. 44:71–90.

Hayes CS, Koskiniemi S, Ruhe ZC, Poole SJ, Low DA. 2014. Mechanisms and biological roles of contact-dependent growth inhibition systems. Cold Spring Harb Perspect Med. 4:a010025.

Heussler GE, et al. 2015. Clustered regularly interspaced short palindromic repeat-dependent, biofilm-specific death of *Pseudomonas aeruginosa* mediated by increased expression of phage-related genes. MBio 6:e00129–15.

Heymann JB, et al. 2013. Three-dimensional structure of the toxin-delivery particle antifeeding prophage of *Serratia entomophila*. J Biol Chem. 288:25276–25284.

Hibbing ME, Fuqua C, Parsek MR, Peterson SB. 2010. Bacterial competition: surviving and thriving in the microbial jungle. Nat Rev Microbiol. 8:15–25.

Hitchcock PJ, Brown TM. 1983. Morphological heterogeneity among *Salmonella* lipopolysaccharide chemotypes in silver-stained polyacrylamide gels. J Bacteriol. 154:269–277.

Hockett KL, Renner T, Baltrus DA. 2015. Independent co-option of a tailed bacteriophage into a killing complex in *Pseudomonas*. MBio 6:e00452–15.

Huang SL, Chen H, Hu A, Tuan NN, Yu CP. 2014. Draft genome sequence of *Pseudomonas nitroreducens* strain TX1, which degrades nonionic surfactants and estrogen-like alkylphenols. Genome Announc. 2:e01262–13.

Hurst MR, Glare TR, Jackson TA. 2004. Cloning *Serratia entomophila* antifeeding genes—a putative defective prophage active against the grass grub *Costelytra zealandica*. J Bacteriol. 186:5116–5128.

Jabrane A, et al. 2002. Characterization of serracin P, a phage-tail-like bacteriocin, and its activity against *Erwinia amylovora*, the fire blight pathogen. Appl Environ Microbiol. 68:5704–5710.

Jeon J, Kim JW, Yong D, Lee K, Chong Y. 2012. Complete genome sequence of the bacteriophage YMC01/01/P52 PAE BP, which causes lysis of verona integron-encoded metallo-beta-lactamase-producing, carbapenem-resistant *Pseudomonas aeruginosa*. J Virol. 86:13876–13877.

Kageyama M, Shinomiya T, Aihara Y, Kobayashi M. 1979. Characterization of a bacteriophage related to R-type pyocins. J Virol. 32:951–957.

Katoh K, Standley DM. 2013. MAFFT multiple sequence alignment software version 7: improvements in performance and usability. Mol Biol Evol. 30:772–780.

Kawato Y, et al. 2015. Complete genome sequence analysis of two *Pseudomonas plecoglossicida* phages, potential therapeutic agents. Appl Environ Microbiol. 81:874–881.

Kim M, Heu S, Ryu S. 2014. Complete genome sequence of enterobacteria phage 4MG, a new member of the subgroup "PVP-SE1-like phage" of the "rV5-like viruses." Arch Virol. 159:3137–3140.

Kocíncová D, Lam JS. 2013. A deletion in the wapB promoter in many serotypes of *Pseudomonas aeruginosa* accounts for the lack of a terminal glucose residue in the core oligosaccharide and resistance to killing by R3-pyocin. Mol Microbiol. 89:464–478.

Koeuth T, Versalovic J, Lupski JR. 1995. Differential subsequence conservation of interspersed repetitive *Streptococcus pneumoniae* BOX elements in diverse bacteria. Genome Res. 5:408–418.

Köhler T, Donner V, van Delden C. 2010. Lipopolysaccharide as shield and receptor for R-pyocin-mediated killing in *Pseudomonas aeruginosa*. J Bacteriol. 192:1921–1928.

Lan SF, et al. 2009. Characterization of a new plasmid-like prophage in a pandemic *Vibrio parahaemolyticus* O3:K6 strain. Appl Environ Microbiol. 75:2659–2667.
Lee M, et al. 2013. Cell-wall remodeling by the zinc-protease AmpDh3 from *Pseudomonas aeruginosa*. J Am Chem Soc. 135:12604–12607.
Leiman PG, Shneider MM. 2012. Contractile tail machines of bacteriophages. Adv Exp Med Biol. 726:93–114.
Li W, et al. 2011. Promysalin, a salicylate-containing *Pseudomonas putida* antibiotic, promotes surface colonization and selectively targets other *Pseudomonas*. Chem Biol. 18:1320–1330.
Li W, et al. 2013. The antimicrobial compound xantholysin defines a new group of *Pseudomonas* cyclic lipopeptides. PLoS One 8:e62946.
Lifshitz RJ, et al. 1987. Growth promotion of canola (rapeseed) seedlings by a strain of *Pseudomonas putida* under gnotobiotic conditions. Can J Microbiol. 33:390–395.
Liu J, Chen P, Zheng C, Huang YP. 2013. Characterization of maltocin P28, a novel phage tail-like bacteriocin from *Stenotrophomonas maltophilia*. Appl Environ Microbiol. 79:5593–5600.
Loper JE, et al. 2012. Comparative genomics of plant-associated *Pseudomonas* spp.: insights into diversity and inheritance of traits involved in multitrophic interactions. PLoS Genet. 8:e1002784.
Makhov AM, et al. 1993. The short tail-fiber of bacteriophage T4: molecular structure and a mechanism for its conformational transition. Virology 194:117–127.
Martínez-García E, Jatsenko T, Kivisaar M, de Lorenzo V. 2015. Freeing *Pseudomonas putida* KT2440 of its proviral load strengthens endurance to environmental stresses. Environ Microbiol. 17:76–90.
Mavrodi DV, Loper JE, Paulsen IT, Thomashow LS. 2009. Mobile genetic elements in the genome of the beneficial rhizobacterium *Pseudomonas fluorescens* Pf-5. BMC Microbiol. 9:8.
McCaughey LC, et al. 2014. Lectin-like bacteriocins from *Pseudomonas* spp. utilise D-rhamnose containing lipopolysaccharide as a cellular receptor. PLoS Pathog. 10:e1003898.
Metelev M, Serebryakova M, Ghilarov D, Zhao Y, Severinov K. 2013. Structure of microcin B-like compounds produced by *Pseudomonas syringae* and species specificity of their antibacterial action. J Bacteriol. 195:4129–4137.
Michel-Briand Y, Baysse C. 2002. The pyocins of *Pseudomonas aeruginosa*. Biochimie. 84:499–510.
Miyazaki R, et al. 2014. Comparative genome analysis of *Pseudomonas knackmussii* B13, the first bacterium known to degrade chloroaromatic compounds. Environ Microbiol. 17:91–104.
Mobberley JM, Authement RN, Segall AM, Paul JH. 2008. The temperate marine phage ΦHAP-1 of *Halomonas aquamarina* possesses a linear plasmid-like prophage genome. J Virol. 82:6618–6630.
Morales-Soto N, Gaudriault S, Ogier JC, Thappeta KR, Forst S. 2012. Comparative analysis of P2-type remnant prophage loci in *Xenorhabdus bovienii* and *Xenorhabdus nematophila* required for xenorhabdicin production. FEMS Microbiol Lett. 333:69–76.
Mutschler H, Meinhart A. 2011. ε/ζ systems: their role in resistance, virulence, and their potential for antibiotic development. J Mol Med (Berl). 89:1183–1194.
Nakayama K, Kanaya S, Ohnishi M, Terawaki Y, Hayashi T. 1999. The complete nucleotide sequence of ϕCTX, a cytotoxin-converting phage of *Pseudomonas aeruginosa*: implications for phage evolution and horizontal gene transfer via bacteriophages. Mol Microbiol. 31:399–419.
Nakayama K, et al. 2000. The R-type pyocin of *Pseudomonas aeruginosa* is related to P2 phage, and the F-type is related to lambda phage. Mol Microbiol. 38:213–231.
Nielsen TH, Cristophersen C, Anthoni U, Sørensen J. 1999. Viscosinamide, a new cyclic depsipeptide with surfactant and antifungal properties produced by *Pseudomonas fluorescens* DR54. J Appl Microbiol. 87:80–90.
Parret AH, Schoofs G, Proost P, De Mot R. 2003. Plant lectin-like bacteriocin from a rhizosphere-colonizing *Pseudomonas* isolate. J Bacteriol. 185:897–908.
Parret AH, Temmerman K, De Mot R. 2005. Novel lectin-like bacteriocins of biocontrol strain *Pseudomonas fluorescens* Pf-5. Appl Environ Microbiol. 71:5197–5207.
Rangel G, Kutter E, Vives M. 2013. Genome sequence of the new *Pseudomonas aeruginosa* temperate bacteriophage PAN70. Paper presented at 20th Biennial Evergreen International Phage Meeting, August 4–9, 2013. Olympia, WA.
Rokni-Zadeh H, et al. 2012. Genetic and functional characterization of cyclic lipopeptide white-line-inducing principle (WLIP) production by rice rhizosphere isolate *Pseudomonas putida* RW10S2. Appl Environ Microbiol. 78:4826–4834.
Roy PH, et al. 2010. Complete genome sequence of the multiresistant taxonomic outlier *Pseudomonas aeruginosa* PA7. PLoS One 5:e8842.
Ruhe ZC, Low DA, Hayes CS. 2013. Bacterial contact-dependent growth inhibition. Trends Microbiol. 21:230–237.
Russell AB, Peterson SB, Mougous JD. 2014. Type VI secretion system effectors: poisons with a purpose. Nat Rev Microbiol. 12:137–148.
Saier MH Jr, Reddy BL. 2015. Holins in bacteria, eukaryotes, and archaea: multifunctional xenologues with potential biotechnological and biomedical applications. J Bacteriol. 197:7–17.
Sarris PF, Ladoukakis ED, Panopoulos NJ, Scoulica EV. 2014. A phage tail-derived element with wide distribution among both prokaryotic domains: a comparative genomic and phylogenetic study. Genome Biol Evol. 6:1739–1747.
Shikuma NJ, et al. 2014. Marine tubeworm metamorphosis induced by arrays of bacterial phage tail-like structures. Science 343:529–533.
Shinomiya T. 1984. Phenotypic mixing of pyocin R2 and bacteriophage PS17 in *Pseudomonas aeruginosa* PAO. J Virol. 49:310–314.
Shinomiya T, Ina S. 1989. Genetic comparison of bacteriophage PS17 and *Pseudomonas aeruginosa* R-type pyocin. J Bacteriol. 171:2287–2292.
Smarda J, Benada O. 2005. Phage tail-like (high-molecular-weight) bacteriocins of *Budvicia aquatica* and *Pragia fontium* (Enterobacteriaceae). Appl Environ Microbiol. 71:8970–8973.
Soares-Castro P, Santos PM. 2013. Towards the description of the genome catalogue of *Pseudomonas* sp. strain M1. Genome Announc. 1:e00146–12.
Strauch E, et al. 2001. Characterization of enterocoliticin, a phage tail-like bacteriocin, and its effect on pathogenic *Yersinia enterocolitica* strains. Appl Environ Microbiol. 67:5634–5642.
Summer EJ, et al. 2007. Rz/Rz1 lysis gene equivalents in phages of Gram-negative hosts. J Mol Biol. 373:1098–1112.
Sun Z, et al. 2014. PrtR homeostasis contributes to *Pseudomonas aeruginosa* pathogenesis and resistance against ciprofloxacin. Infect Immun. 82:1638–1647.
Sundin GW, Jacobs JL, Murillo J. 2000. Sequence diversity of *rulA* among natural isolates of *Pseudomonas syringae* and effect on function of *rulAB*-mediated UV radiation tolerance. Appl Environ Microbiol. 66:5167–5173.
Thaler JO, Baghdiguian S, Boemare N. 1995. Purification and characterization of xenorhabdicin, a phage tail-like bacteriocin, from the lysogenic strain F1 of *Xenorhabdus nematophilus*. Appl Environ Microbiol. 61:2049–2052.
Touchon M, Bobay LM, Rocha EP. 2014. The chromosomal accommodation and domestication of mobile genetic elements. Curr Opin Microbiol. 22:22–29.
Toyofuku M, et al. 2014. Membrane vesicle formation is associated with pyocin production under denitrifying conditions in *Pseudomonas aeruginosa* PAO1. Environ Microbiol. 16:2927–2938.
Vlassak K, Van Holm L, Duchateau L, Vanderleyden J, De Mot R. 1992. Isolation and characterization of fluorescent *Pseudomonas* associated

with the roots of rice and banana grown in Sri Lanka. Plant Soil 145:51–63.

Weller DM, Cook RJ. 1983. Suppression of take-all of wheat by seed treatments with fluorescent pseudomonads. Phytopathology 73:463–469.

Williams SR, Gebhart D, Martin DW, Scholl D. 2008. Retargeting R-type pyocins to generate novel bactericidal protein complexes. Appl Environ Microbiol. 74:3868–3876.

Winsor GL, et al. 2011. *Pseudomonas* Genome Database: improved comparative analysis and population genomics capability for *Pseudomonas* genomes. Nucleic Acids Res. 39:D596–D600.

Wu W, Jin S. 2005. PtrB of *Pseudomonas aeruginosa* suppresses the type III secretion system under the stress of DNA damage. J Bacteriol. 187:6058–6068.

Wu X, et al. 2011. Comparative genomics and functional analysis of niche-specific adaptation in *Pseudomonas putida*. FEMS Microbiol Rev. 35:299–323.

Yamada K, et al. 2006. Nucleotide sequences and organization of the genes for carotovoricin (Ctv) from *Erwinia carotovora* indicate that Ctv evolved from the same ancestor as *Salmonella typhi* prophage. Biosci Biotechnol Biochem. 70:2236–2247.

Yang G, Dowling AJ, Gerike U, ffrench-Constant RH, Waterfield NR. 2006. *Photorhabdus* virulence cassettes confer injectable insecticidal activity against the wax moth. J Bacteriol. 188:2254–2261.

Young R. 2014. Phage lysis: three steps, three choices, one outcome. J Microbiol. 52:243–258.

Zhang Y, Yamaguchi Y, Inouye M. 2009. Characterization of YafO, an *Escherichia coli* toxin. J Biol Chem. 284:25522–25531.

Zink R, Loessner MJ, Scherer S. 1995. Characterization of cryptic prophages (monocins) in *Listeria* and sequence analysis of a holin/endolysin gene. Microbiology 141:2577–2584.

Associate editor: Howard Ochman